UNIVERSITÀ DEGLI STUDI DI PADOVA

DIPARTIMENTO DI INGEGNERIA INDUSTRIALE

CORSO DI LAUREA MAGISTRALE IN INGEGNERIA CHIMICA E DEI PROCESSI INDUSTRIALI

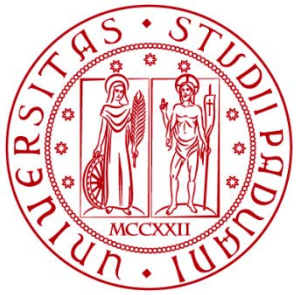

Tesi di Laurea Magistrale in Ingegneria Chimica e dei Processi Industriali

OPERANDO FT-IR INVESTIGATION OF SURFACE REACTIONS IN TRANSIENT REGIME

Relatore: Prof. Paolo Canu
Correlatore: Prof. Christophe Dujardin

Laureanda: GIULIA SCHIONATO
Matricola: 1154685

ANNO ACCADEMICO 2018-2019

Abstract

This work of thesis focuses on the use of *operando* FT-IR spectroscopy to investigate the toluene total oxidation mechanism occurring onto the surface of a $Pt/\gamma\text{-}Al_2O_3$ commercial catalyst. The effect of the Pt oxidative state and sintering due to catalyst aging has been studied and compared.

The experiments have been performed from an industrial perspective: a commercial catalyst for VOC treatment has been used and the catalyst mass/reactant ratio (w/F) has been kept as lower as possible to simulate car exhaust combustion conditions.

The performance studies have highlighted that the oxidative state of Pt had a negligible effect on catalytic activity. Instead, the aged catalyst has shown an activity decrease.
Operando FT-IR experiments have led to an hypothesis of main reaction pathway, in which, after its adsorption, toluene is sequentially oxidized to benzoate, aliphatic carboxylates species, CO and, finally, CO_2. In this mechanism, the rate determining is represented by the decomposition of benzoate species, which are also the main intermediates of the reaction.

Table of Contents

List of Figures

List of Tables

Introduction

Heterogeneous catalysis is ever-present in people life. Actually, catalysts lie in the heart of petroleum-refinery and chemical industry since most products (about 90%) are produced through catalytic processes [1]. They also play a key role in the abatement of car and industrial exhaust [2][3].

Despite their wide spread diffusion, there are still questions on how reactants are transformed into product over a specific catalyst [4]. In fact, catalytic reactions display a very complicated dynamics due to the occurrence of numerous steps inside the reaction cycle.

Therefore, obtaining reliable insights on reaction mechanism and understanding the structure-activity relationship become a very attractive challenge in the catalyst field. Giving an answer to these questions would allow the improvement of existing catalysts or the design of more efficient ones.

One of the latest and most promising methodologies to investigates the dynamics of a catalytic process is *operando* spectroscopy. This technique combines time resolved *in situ* spectroscopy and online product analysis. Thus, it makes possible to correlate the evolution of adsorbed species on catalyst surface with catalyst performances (conversion and selectivity) under relevant reaction conditions.

The purpose of this work is to use *operando* FT-IR spectroscopy to study the reaction steps occurring on the surface of a commercial Pt-based catalyst during the total toluene oxidation (chosen as a model reaction). Several catalyst conditions are investigated to evaluate the effect of the Pt oxidative state and sintering on the evolution of the reaction.

Thesis Structure

The first chapter gives an overview on the *operando* spectroscopy methodology. First, a brief evolution of spectroscopic approaches is reported together with some pioneer studies. Then the concept of *operando* spectroscopy with regard to the reaction cycle investigation and its requirements are presented. A literature review of the chosen model reaction is also reported.

In the second chapter the experimental set up and analysis instruments are described. The tests were performed in a homemade *operando* set up where the evolution of the species and the product composition were monitored with FT-IR spectroscopy and a GC-MS, respectively. The chapter presents the set up, the materials and the operating condition for the work.

In the final chapter, all the results are reported and discussed in detail. The catalytic performances, as well as the determination of reaction controlling regime are firstly presented. Then the FT-IR spectra and *operando* investigation are discussed focusing on the evolution of adsorbed species over the catalytic surface, giving valuable indication on a possible reaction cycle.

This thesis is the result of the collaboration between the Industrial Engineering Department of University of Padua and the Catalysis and Solid Chemistry Unit (UCCS) of Ecole Nationale Supérieure de Chimie of Lille (France). The experimental activities were carried out in the UCCS laboratories.

Chapter 1

Operando spectroscopy

Nowadays, heterogenous catalysis plays a major role in society considering that over 85% of chemical products have been in contact with at least one catalyst in their production chain. Catalytic processes are also required to reduce the environmental pollution from car and industrial exhaust gases [2][3]. Thus, understanding more deeply the mechanistic insights on catalytic processes represents one of the most relevant accomplishment to develop new or improve catalysts for a more sustainable society.

In particular, whit the aim of investigating the structure-activity relationship at molecular and atomic scale, *Operando* spectroscopy represents one of the most cutting-edge tools available at this time because it makes possible to perform spectro-kinetic measurements under real reaction conditions.

1.1 Spectroscopic analysis over the years

Generally, catalytic processes show a very complex dynamics. Actually, this processes complexity is the result of numerous consequent-parallel elementary steps, which form the main reaction cycle, and the formation, deactivation and reactivation of active species, which do or do not participate in the main catalytic cycle [5][6]. Therefore, the development of physical or physiochemical approaches and methods able to collect trustworthy data on global reaction mechanisms always represent a step forward in the catalytic research field. Without any doubt, spectroscopic investigations consistently influenced the progress in catalysis development [7].

In the early studies, all the catalytic spectroscopic investigations were performed *ex situ* (from Latin “off-site”, “from site”). The catalysts state were analyzed only before (fresh catalysts/catalyst precursors) and after (spent catalysts) the reactions occurrence [6][8]. However, despite their importance, the obtained data provided only partial information to understand industrial processes because *ex situ* studies not allow to reveal reliable insights on the real dynamic of the reactions [9].

Therefore, the natural improvement in this field was to adapt spectroscopic techniques to monitor the physiochemical process occurring on the catalyst during an ongoing reaction, under relevant operating conditions [10]. This methodology is called *in situ* spectroscopy (from Latin

"on position", "on site"). The first attempt to implement this technique dating back to the 1950s when R. P. Eischens and others [11][12] investigated the CO interactions with Cu, Pt, Pd and Ni supported on SiO_2 and NH_3 interactions with cracking catalysts with IR spectroscopy. Undoubtedly, these studies cannot be considered as real *in situ* spectroscopic applications, but these researchers were the firsts to actual stress on the relevance of the catalytic surface dynamics to obtain a more complete investigation of reactions.
Since these first attempts, *in situ* spectroscopy has shown a continuous progress in the catalyst field together with a rapid increase of publications starting from the 1980s as shown in ***Figure 1.1.1***.

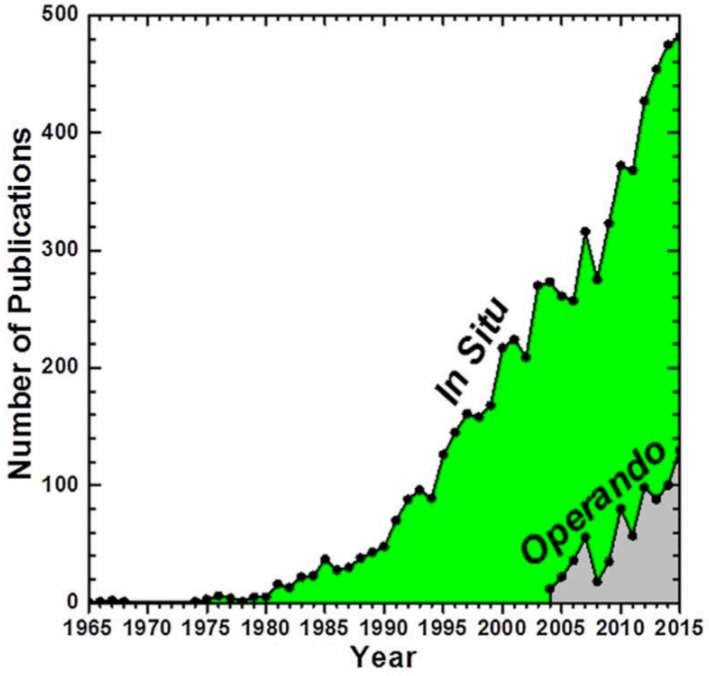

Figure 1.1.1 *Number of catalysis publication per years utilizing in situ or operando spectroscopy characterization [13].*

Initially, studies adopting *in situ* spectroscopic methodologies investigated reactions occurring under model conditions, meaning at high catalyst/reactant ratio, in presence of ligands and absences of catalytic system components and under not optimal operating conditions for the reaction. Moving forward with technology improvements, scientists also have been able to make spectroscopic investigations under actual reaction conditions. Therefore, obtain reliable information on changes in the catalyst structure and surface species during the reactant-to-product conversion has become possible.

Nowadays, *in situ* spectroscopic measurements under real reaction conditions can be performed with several techniques:

- Raman spectroscopy [13]: technique which provides information on the molecular structure of the solid support of the catalyst, in particular it has been applied to investigate the main properties of catalytic materials (bulk and supported metals, metal oxides, sulfides, etc.);
- IR spectroscopy (FTIR, DRIFT, ATR-IR, PM-IRRA) [14]: techniques which investigate the presence of any functional group in the catalyst sample; generally, absorption or reflection spectra are used, and both provides information about the surface properties, structure, adsorbed species, etc.;
- *UV-vis* spectroscopy [15][16]: this technique is adopted for monitoring both the dissolved molecular species and the size of nanoparticles;
- NMR spectroscopy [17][18]: technique used to study the molecular conformation as well as physical properties at molecular level in solution.

In the light of above, it seems clear that *in situ* spectroscopy by itself represents a powerful tool to observe catalysts surface modifications under controlled conditions.

However, this methodology is still insufficient to provide a direct correlation between catalysts structure (surface) and corresponding reaction performance (conversion and selectivity) due to the lack of a reaction products analysis.

To overcome this limitation, a cutting-edge approach has been proposed. It simultaneously combines time resolved *in situ* spectroscopy and online product analysis under real reaction conditions. This methodology in the scientific field is known as *operando* spectroscopy [19]. The term *operando* is taken from Latin and means "working" or "operating" and it was introduced in literature for the first time by M. A. Bañares and its group in 2002 [13][20][21]. With this single word M. A. Bañares has been able to underline the simultaneous evaluation of the catalytic surface structure (active sites, adsorbed species, etc.) and reaction performances achieved with this technique [19].

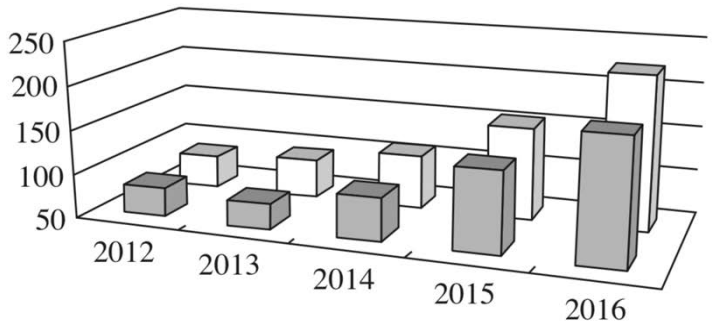

Figure 1.1.2 *Number of publications containing the term 'operando spectroscopy' in titles, abstracts, or keywords, as index in the Web of Science (white) and Scopus (grey) in 2012-2016 [7].*

Since that year, *operando* spectroscopy has gained ever-increasing popularity for investigating catalytic reactions mechanisms, as detected also by the growing number of publications on this topic in literature (***Figure 1.1.1***-**Figure 1.1.2**). All facts that underlines the keen importance of *operando* spectroscopy applied to the catalytic reaction mechanism.

1.1.1 Early operando IR studies

Before 2002, when the term *operando* has been coined [20], it is difficult to outline if the *operando* IR experimental set up has been used in heterogeneous catalysis because of the absence of references in literature. However, there are some avant-guard studies which have contributed to the development of this approach.

In 1968, J. W. Ward used an IR cell reactor working as a flow reactor to record spectra of the catalyst (ammonium Y Zeolite) during cumene cracking through the cell. In addition, the outlet stream was simultaneously monitored by gas chromatography [22]. However, the study did not report any catalytic data, thus the full potential of the set up hasn't been exploited.

In 1991, a combination of IR spectroscopy and gas chromatographic analysis of the effluents is used by Joly et al. to characterize the active sites of dealuminated HY zeolites during the conversion of cyclohexane. Moreover, the sites responsible for the catalytic activity and coke formation are determinate thanks to this configuration [23].

Three years later, in 1994, in situ IR spectroscopy together with the gas chromatographic analysis is adopted to investigate the butyne hydrogenation on a Pt/silica catalyst [24].

Lastly, a review by J. Saussey et al. reported a work by Freyez et al. who used in situ IR spectroscopy combined with the investigation of the outlet stream composition with mass spectroscopy to outline the role of CO in NO_x reduction on Pt/silica catalysts [25]. With this configuration, the researchers were able to define the rate determining step of the reaction and to affirm that there is no direct reaction between NO and CO, in contrast with previously assumptions.

1.2 The *operando* spectroscopy idea

Back in 2005, when M. A. Bañares outlined the main points of *operando* methodology [19], *operando* spectroscopy referred to the methodology resulting from the simultaneous combination of *in situ* spectroscopy and online kinetic measurements of the catalytic system under actual reaction condition. In other words, spectroscopy together with online product analysis are used to derivate information on the relation between structure (composition) and catalyst performances (conversion or selectivity) [1][13].

The catalytic activity can be evaluated through both reaction conversion X (or selectivity) and apparent reaction rate constant k_{app} (or activation energy). The former is defined in Eq. 1.1; the latter is a proportional constant which relates the reaction rate to the reactant amount (Eq. 1.2) [13][19]. It is called 'apparent' rate constant because the catalytic reaction complexity, due to the numerous steps involved, makes practically impossible the determination of all involved rate constants [7].

$$X = \frac{amount\ of\ consumed\ reactant}{amount\ of\ fed\ reactant} \tag{1.1}$$

$$R = k_{app}[reactants\ amount]^n \tag{1.2}$$

Determining at least one of these relationships is necessary to achieve the final objective of *operando* studies, i.e. obtaining fundamental insights on the structure-activity relationship [13][19]. Although, these data alone are not enough.

The currently knowledge in the catalysis field does not leave any doubt that when a reaction occurs not only active but also inactive species are involved and present among the products. Nevertheless, this fact rarely is taken into account in *operando* discussions even if the inactive species are just as relevant as active ones in catalysts performances evaluations. Inactive species affect the composition of the end product mixture and consequently the catalyst selectivity.

As the reaction proceed, the amount of active and inactive species may vary significantly affecting not only the activity but also the structure of catalysts. Thus, a time-resolved analysis of the variation of the species on the catalyst is required to make possible a definition of structure-activity correlation and to have an idea of active/inactive species involved.

To obtain this relationship, as said before, *operando* spectroscopy is very helpful tool. Online product analysis instruments (e.g. MS, GC, etc.) provide data on catalyst activity and help to evaluate potential reaction intermediates or byproducts. Meanwhile, *in situ* spectroscopic techniques (e.g. Raman, IR, etc.) give information on how reactants are converted in to products, monitoring the evolution of the species on the catalyst surface.

Combining these data together information on the reaction pathway are obtained comprehensive of the discrimination between active and inactive species involved.

1.2.1 Goals and tasks

As stated several times by now, the main goal of *operando* spectroscopy is to point out the structure-activity relationship. To achieve this result, different tasks should be solved which can be reconducted into two main groups, closely related to each others.

The first group tasks aim at obtaining new crucial insights on the complete mechanism of a catalytic system, with a precise identification of the role of the involved species. Whereas, the ones of the second group focus on the chemical and automotive industry needs, taking into account already known catalytic processes and optimizing them. It is clear that from the academic point of view the first group represents the most interesting research field.

The above knowledge on complete catalytic system mechanism means not only the determination of main catalytic cycle (the biggest contribution for the formation of the desired reaction products) but also the catalytic transformations occurring outside the main reaction catalytic cycle because they affect the catalyst activity and selectivity as well. The knowledge of these processes allows to determinate the actual activity of the catalyst and finally define its selectivity.

A key aspect in *operando* spectroscopic studies is the quality of the data obtained from which depend the reaction model reliability.[14]. In the specific case, the reliable data lack can be caused by missing detection of some components present in the product mixture due to mainly two reasons: they exist in an ultra-low concentration, thus, the instrument is not able to detect them; or the detection method does not fulfill possible component outputs of the catalytic system investigated, so the instrument does not research these particular ones.

In both circumstances, the same problem arises: the contribution of several compounds is ignored in the material balances even if they are important in the reaction mechanism. To overcome these practical issues, more measurements as possible should be taken and instruments as sensible as possible should be used both for the IR spectroscopy and the online product investigation [26][27].

To achieve the ultimate objective of *operando* spectroscopy it is also necessary to manage the technical problems related to the simultaneous identification and monitoring of intermediates and products of both the main catalytic cycle and the transformations happen outside it. Thus, two kind of data are gained: as type 1 data are obtained from the transformations in the main catalytic cycle under real reaction conditions are considered, while type 2 data are those data coming from the transformation caused by the outside processes [7]. In particular, type 1 data provides information on the reaction mechanism that from the reactants leads to the ultimate products, while type 2 data are useful to determinate the role of species in the considered catalytic system.

In the light of above considerations, the acquisition of type 1 data and type 2 and them correlation is the most important experimental mission in *operando* spectroscopy. To achieve this goal, modifications on standard *in situ* experimental set up are needed to enable. In particular, from the practical point of view, the set up requires reactors that make possible concurrent *in situ* spectroscopic analysis and time-resolved online product analysis and that allow to reproduce the same conditions of industrial reactors [14][28][29][30].

1.2.2 The operando spectroscopy set up and requirements

As mentioned above, the *operando* spectroscopy set up represents a key factor for obtaining reliable data. The research on this particular subject is constantly evolving due to *operando* still short background.

Reactor systems used for simple *in situ* spectroscopic analysis are not enough for *operando* investigations because they work at lower operating conditions compared to the industrial reactions. Thus, these systems are stressed to operate in the desired conditions [31][32][33]. In ***Figure 1.2.1*** a schematic representation of *operando* experimental setup is reported.

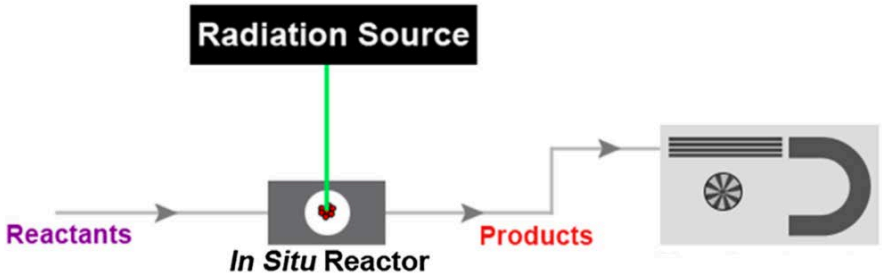

Figure 1.2.1 *Schematic representation of Operando experimental set up [31]..*

In the reported set up (***Figure 1.2.1***), the reactants are sent to an *in situ* IR cell reactor which is coupled with an optical spectrometer to allow time-resolved measurements of the catalytic sample during the reaction. At the same time, the outlet stream is analyzed by analysis instruments in real time.

Despite its theoretical simplicity, the set up is very delicate since many components are connected together. This leads to the possibility of leaks in the system. In particular, they are usually present before the entrance to the analysis instruments.

Nevertheless, the set up power lays in the simultaneous employment of different analysis techniques capable of providing correlation between catalyst activity/structure and reaction intermediates.

1.2.2.1 The *operando* reactor

As mentioned in several occasions, the reactor used in the set up should allow both the *in situ* characterization of the catalytic sample through a spectroscopic technique and the simulation of real industrial processes conditions. However, not all *in situ* reactor cell can be adopted for *operando* studies because the majority of these kind of reactors is not designed for working under 'operando' conditions, e.g. under real or relevant reaction conditions for industrial applications. In fact, a lot of *in situ* reactors are planned to work as batch reactors, which of course can provide interesting information, but the reaction conditions are a long way off the conditions present in real processes.

On the other hand, industrial processes usually work with plug flow reactors. Therefore, data obtained from batch experiments are not relevant due to the stagnation of reactants in the reactor which may causes readsorption of reaction intermediates [31].

Moreover, reactors for *operando* studies should have low dead volume, good reactant-catalyst contact during the reaction, variable space velocity and a uniform as possible temperature profile to conduct isothermal experiments [34].

To fulfill these characteristics usually sandwich cell are used, which consist in cylinder where the catalyst is placed in the middle. The empty space in the cylinder is filled with transparent windows to let the beam see the sample. The rector is therefore put inside an oven for controlling the temperature during the reaction (***Figure 1.2.2***).

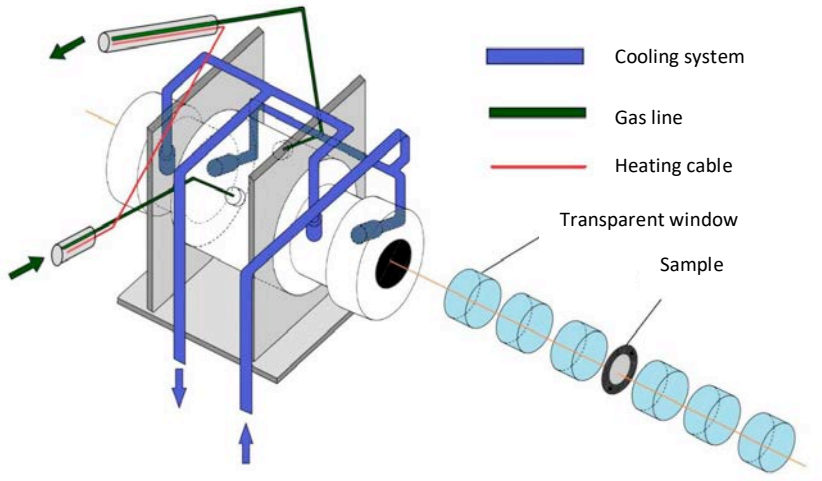

Figure 1.2.2 *IR Reactor scheme*

In addition, to reproduce as similar as possible realistic reaction conditions, the catalyst mass/reactant amount ratio (w/F) should be monitored. In fact, this ratio should be as lower as possible to obtain as realistic as possible reaction conditions. However, decreasing to much this ratio, the quality of the spectroscopic data can be negatively affected due to the overcoming of the instruments detection limits [7]. Example of the influence of w/F ratio are related mainly to the catalyst transformations outside the main reaction cycle as reported in literature [5][35][36].

1.2.2.2 Characterizations techniques

Since 2002 [20], *operando* studies have been performed combining together many spectroscopic techniques for catalyst characterization (Raman, IR, X-Ray, etc.) with online product analysis (MS, GC, EELS, etc.), **Figure 1.2.3** Diagram of operando spectroscopy

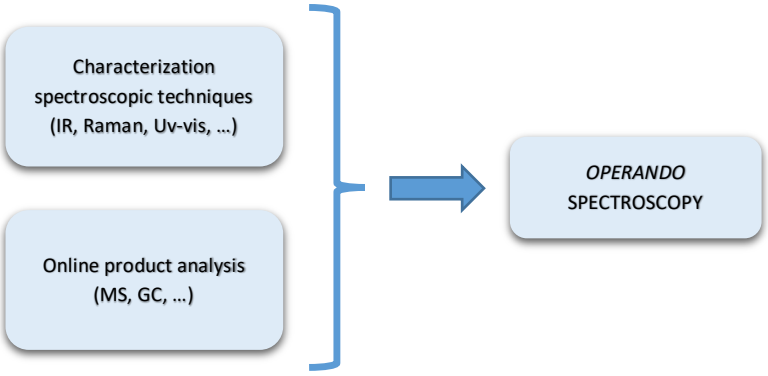

Figure 1.2.3 *Diagram of operando spectroscopy*

Table 1.2.1 reports the first studies where the term '*operando*' is adopted, and the techniques used are pointed out. The first three articles refer to the pioneer studies by M. A. Bañares et al. [13][23][21], where the term *operando* appears. Initially, *Raman* spectroscopy was chosen for the catalyst characterization together with online product analysis with a gas chromatographer. A literature review outlines also that there are techniques which haven't been exploited for *operando* studies yet, e.g. Mössbauer spectroscopy and Sum Frequency Generation (SFG), well established characterization techniques known for decades [31].

Table 1.2.1 *Chronology of the first use of 'operando' together with a specific spectroscopic characterization. Table adapted from [31].*

Catalyst Characterization	*Product Analysis*	Publication Title	Authors	Years
Raman spectroscopy	GC	Operando Raman study of alumina-supported Sb-V-O catalyst during propane ammoxidation to acrylonitrile with online activity measurements	M. O. Guerrero-Pérez M. A. Bañares	2002
Raman spectroscopy	GC	Raman spectroscopy during catalytic operations with on-line activity measurement (operando spectroscopy): a method for understanding the active centers of cations supported on porous materials	M. A. Bañares M. O. Guerrero-Pérez J. L. G. Fierro G. G. Cortez	2002
Raman spectroscopy	GC	Molecular structures of supported metal oxide catalysts under different environments	M. A. Bañares I. E. Wachs	2002
IR spectroscopy	MS	Studying the NOx-trap mechanism over a Pt-Rh/Ba/Al_2O_3 catalyst by operando FT-IR spectroscopy	T. Lesage C. Verrier P. Bazin J. Saussey M. Daturi	2003
UV-vis-Raman spectroscopy	MS	Operando spectroscopic investigation of supported metal oxide catalysts by combined time-resolved UV-vis/Raman/on-line mass spectrometry	T. A. Nijhuis S. J. Tinnemans T. Visser B. M. Weckhuysen	2003
ATM-IR spectroscopy	ATR-IR	Operando ATR-FTIR analysis of liquid-phase catalytic reactions: can heterogeneous catalysts be observed?	G. Mul G. M. Hamminga J. A. Moulijn	2004
EPR spectroscopy	GC	Elucidating structure and function of active sites in VOx /TiO_2 catalysts during oxyhydrative scission of 1-butene by in situ and operando spectroscopy	U. Bentrup A. Brückner C. Rüdinger H.-J. Eberle	2004
XAFS-Raman-UV-vis spectroscopy	MS	Adding a third dimension to operando spectroscopy: a combined UV-vis, Raman and XAFS setup to study heterogeneous catalysts under working conditions	A. M. Beale A. M. J. van der Eerden K. Kervinen M. A. Newton B. M. Weckhuysen	2005
NMR spectroscopy	MS	A continuous gas flow MAS NMR probe for operando studies of hydrocarbon conversion on heterogeneous catalysts	V. Sundaramurthy J.-P. Cognec K. Thomas B. Knott F. Engelke C. Fernandez	2006
NAP-XPS	MS	XPS and DRIFTS operando studies of an inverse CeO_2/CuO WGS catalyst: deactivating role of interfacial carbonates in redox activity	A. L. Camara M. Monte A. Martinez-Arias J. C. Conesa	2012
XRD-XAS-Raman Spectroscopy	MS	Application of Operando XAS, XRD, and Raman Spectroscopy for Phase Speciation in Water Gas Shift Reaction Catalysts	A. Patlolla E. V. Carino S. N. Ehrlich E. Stavitski A. I. Frenkel	2012
TEM	EELS	Operando Transmission Electron Microscopy: A Technique for Detection of Catalysis Using Electron Energy-Loss Spectroscopy in the Transmission Electron Microscope	S. Chenna P. A. Crozier	2012

1.2.3 Reaction mechanism investigation

Before making any hypothesis on reaction mechanisms in *operando* spectroscopy, it should be clear what is meant by 'reaction mechanism'.

As reaction mechanism or reaction cycle, two main points are taken into account: on the one hand, the determination of the consequent-parallel steps that from the reactants lead to the products through intermediates formation and, on the other hand, information on both the activity and structure of the species involved in the reaction. It is important to underline, that these two aspects are equally important to a complete description of the mechanism [5].

However, assumptions on the reaction mechanism can be considered reliable as long as it is supported by the observed kinetics [37]. Therefore, it comes clear that kinetic investigation represents the key aspect for determining the reaction mechanism. In particular, the use of the two type of data described in previous section which consider transformation, on both outside and inside the main reaction cycle, is the best way to achieve the main goals of *operando* spectroscopy, e.g. main reaction cycle identification (type 1) and information on the role of observed species (type 2).

All in all, in the catalysis field it is widely accepted that *operando* spectroscopic investigations refer only to the data belonging to type 1: data coming from simultaneous combination of *in situ* spectroscopic investigation of the catalyst surface and online product analysis [13][19].

Therefore, this work focuses the attention on type 1 kinetic data (combination of *in situ* spectroscopic investigation of the catalyst surface and online product analysis) to propose a hypothesis of the main reaction cycle of a model reaction.

1.3 Model reaction

The complete catalytic oxidation (or combustion) of low-concentration VOCs (Volatile Organic Compounds) is considered. In particular, catalytic combustion of toluene (C_7H_8) is chosen as model reaction of VOCs abatement studies because of the extensive emissions of this molecule not only in petroleum and fine chemical industrial activities, but also in car exhausts [2][3][38][39]. The reaction stoichiometry is described by Eq. 2.1.

$$C_7H_8 + 9\,O_2 \rightarrow 7\,CO_2 + 4\,H_2O \qquad (2.1)$$

Regarding the nature of potential catalysts, a literature review shows that this reaction can be carried out on in several catalysts which can roughly divided in two kinds: noble metals (Pt, Pd, Rh) and oxides transition metals (Mn, Co, Cu) [40][41][42]. Since the mixture to the reactor contains only toluene with a 99.9% of purity, a Pt/γ-Al_2O_3 catalyst is adopted in this study. This kind of catalyst shows a very high activity and stability for toluene as long as for several VOCs combustion[43][44][45][46].

Table 1.3.1 *Catalytic performance parameters for toluene combustion over Pt/γ-Al_2O_3 reported in literature*

d_{Pt} [nm]	$C_{toluene}$ [ppm][a]	T_{50} [°C]	T_{90} [°C]	Reference
12	950	185	200	[47]
	242	135	145	[42]
1	1500	178	190	[48]
15.5	1500	190	200	[48]
4.8	300	160	190	[49]

[a] $C_{toluene}$: toluene concentration in the feed gas stream.

Table *1.3.1* summarizes activity results (T_{50} and/or T_{90} - temperatures at which toluene conversion is 50% and 90%, respectively) for toluene combustion over the same catalyst found in literature.

Before researchers have speculated on the toluene combustion mechanism.
G. Busca [50] and G. da Silva et al. [51] have reported that toluene combustion proceeds in consecutive steps via benzylic, aldehydic and benzoate species. S. Besselmann et al. [52] have

investigated the toluene oxidation mechanism on V_2O_5/TiO_2 catalysts and have reported the same reaction steps proposed by the studied above.

Instead, the same reaction occurring on the OMS-2 catalyst has been studied by H. Sun et al. [53]. The researchers pointed out that toluene is adsorbed through its C atoms to the O_2 atoms of the catalyst, an H of the methyl group is abstracted and sequentially benzoyl intermediates are formed. Then, these intermediates are oxidized into aldehydic and benzoate species, which are further oxidized in the final products (CO_2 and H_2O).

S. Zhao et al. [28] have studied the mechanism over a Pd-Co based catalyst concluding that toluene is oxidized to aldehydic species rapidly transformed into benzoate species. They also found that benzoate species are the main intermediates in toluene oxidation and these species are further oxidized with O_2 in the ultimate products.

Toluene combustion mechanism on Pt/TiO_2 catalysts is reported by Z. Rui et al. [54], who have investigated the. They have reported that, once adsorbed, toluene reacts with O_2 and is sequentially transformed in aromatic aldehydic (e.g. benzaldehyde), benzoate, aliphatic carboxylic (e.g. carboxylic acid species) and anhydrides species. The latter are then converted into adsorbed CO species and H_2O. Lastly, the adsorbed CO species react with O_2 to give CO_2. They have discovered that benzoate species are the main intermediates in toluene oxidation on this catalyst (as pointed out by S. Zhao et al.) and that their decomposition is the rate determining step of the reaction.

In general, it can be concluded that in its combustion toluene is sequentially oxidized in benzylic, aldehydic and benzoate species. Then the latter are further converted into the final products (CO_2 and H_2O).

Chapter 2

Experimental Methods

This chapter focuses on the instruments and methodologies adopted for all the experiments. All the experiments have been done in the UCCS (Unité de Catalyse et Chimie de Solide) laboratories, belonging to the Ecole Nationale Supérieure de Chimie de Lille.

2.1 Experimental scheme

All the experiments are conducted in the same laboratory scale *Operando* system connected to a flow set-up as schematically represented in **Figure 2.1.1**.

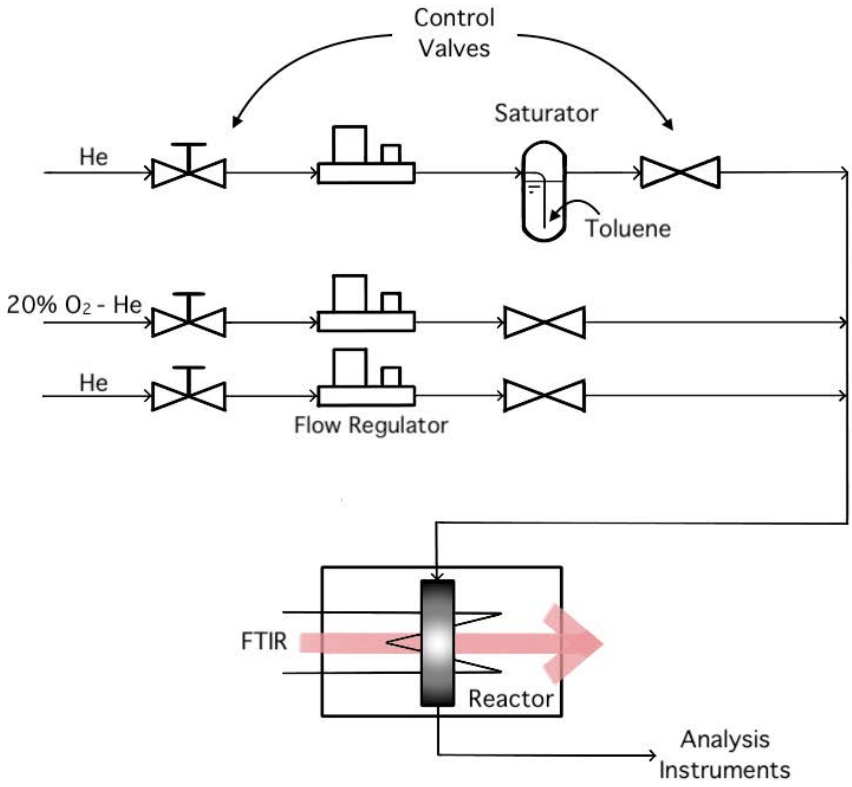

Figure 2.1.1 *Experimental plant set up.*

In this set-up, the exact amount of toluene is delivered to the system in vapor phase via a saturator purged with helium flow as carrier gas. While oxygen and helium are introduced into the lines by mass flow controllers to obtain the exact proportions in the reagent mixture. Thus, the obtained mixture is sent to a sandwich cell reactor, a spectroscopic reactor wildly used on laboratory scale for time-resolved measurements of the catalyst during an on-going reaction. In particular, the evolution of the adsorbed species on the catalyst surface is investigated through a FT-IR spectrometer. Instead, the reaction products exiting the reactor are analyzed by a Quadrupole Mass Spectrometer and a micro-Gas Chromatographer.
In the following paragraphs all components will be described in more details.

2.1.1 Mass Flow Controllers: Brooks Delta SLA5800

To control the reactant flowrates to the reactor, *Brooks Delta SLA5800* mass flow controllers (MFC) are used, **Figure 2.1.1.1**.These devices are able to automatically control gas flowrates according to a set point sent as an electrical signal.

Figure 2.1.1.1 *Brooks Delta SLA5800 mass flow controller.*

The measuring part is comprehensive of a laminar flow element combined with a thermal mass flow sensor, which are filled with gas once the device has been connected to the process line and the valve has been open. A schematic representation of an MFC is reported in **Figure 2.1.1.2**.

The sensor is capillary tube, that by passes the laminar flow element, equipped with a heater and two temperature recorders, one positioned before and the other after the heater. The heater heats the tube and the temperature sensors record the temperature: as long as there is no flow in the by-pass tube, both temperatures equally increase (T_1=T_2) so the measured value is zero ($\Delta T=0$) and the corresponding signal is sent to the micro-processor.
The instrument receives a set point from the analog port which is compared to the measured value. If the latter is lower than the required value, the PID controller will actuate the control valve by opening it. Now, the gas flow is able to pass through the instrument.
The gas flows through the laminar flow element which makes the flow laminar and perfectly predictable. This component is fundamental to calibrate the MFC for any gas and ensures that part of it passes through the sensor. The gas, which is cold, cools down the first temperature recorder ($T_1\downarrow$) while the second one sees that the gas has been heated by the heater ($T_2\uparrow$). Thus, the measured difference in temperature is no longer zero ($\Delta T\neq 0$) and it provides a direct measure for the mass flow according to the energy conservation law. As earlier, the corresponding signal is sent to the micro-processor and compared to the set point and the PID controller will actuate consequently by opening or closing the valve to obtain the desired mass flow.

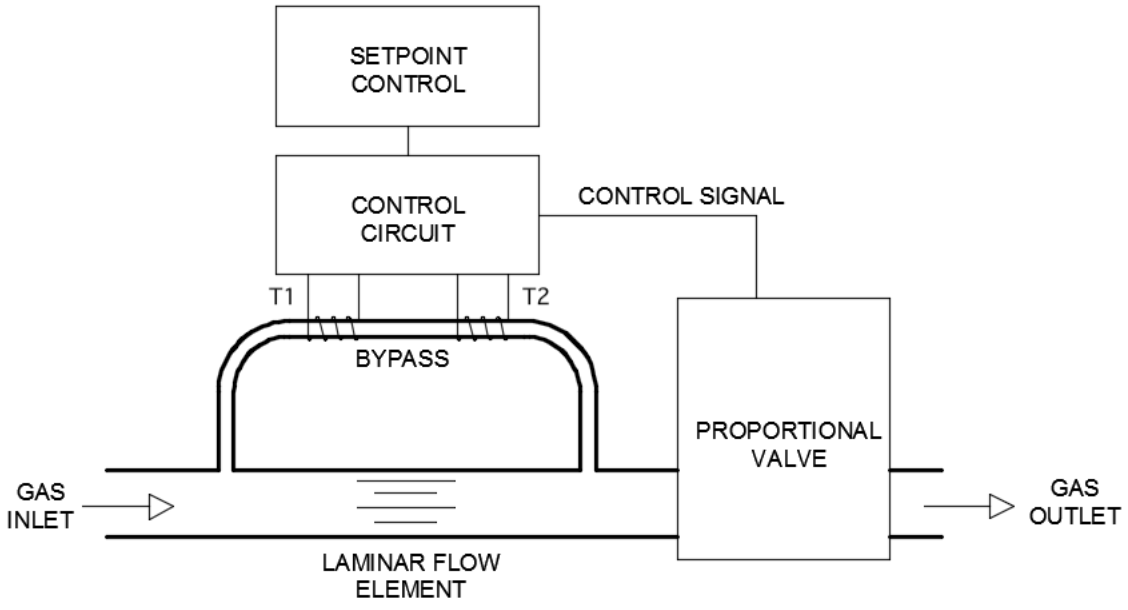

Figure 2.1.1.2 *Mass flow controller working scheme.*

All these operations are performed in few milliseconds in order to obtain a very constant and stable gas flow.

2.1.2 Saturator

A homemade saturator is employed to ensure the desired amount of Toluene in the reaction mixture. It is comprehensive of two parts, as shown in the scheme in **Figure 2.1.2.1**: an evaporator and a cooler, both made out of glass.

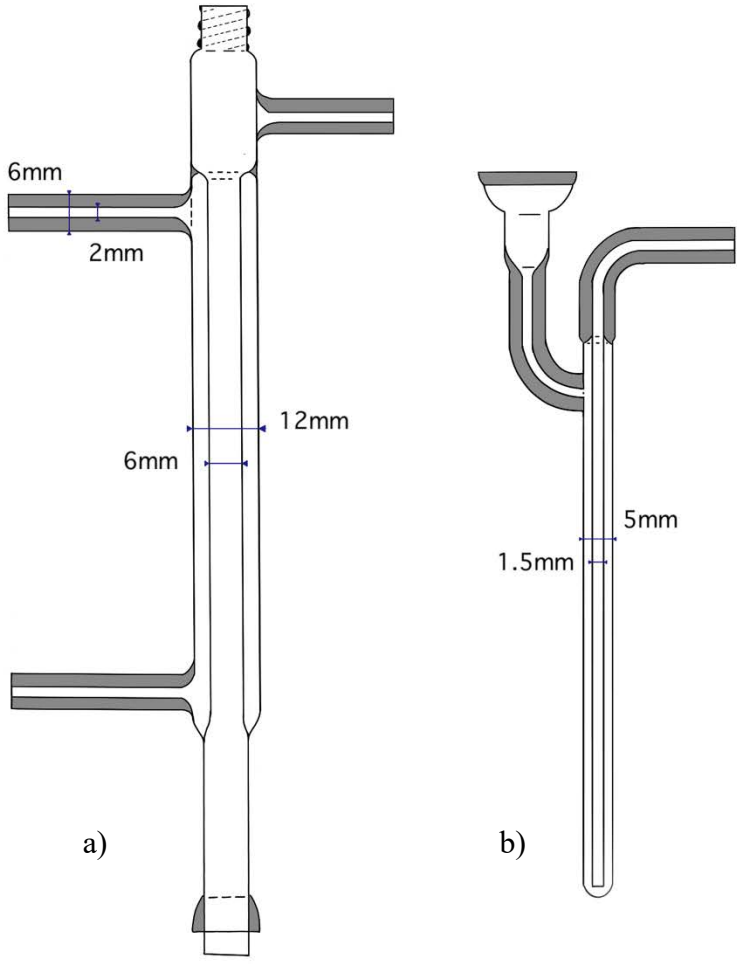

Figure 2.1.2.1 *Saturator scheme: a) cooler, b) evaporator.*

The evaporator (**Figure 2.1.2.1 - a**) consists in a cylinder vessel (5 mm of internal diameter) where 500 mg of 99.9% pure toluene at ambient temperature is placed in order to ensure enough toluene for the duration of at least one experiment. In the center of the cylinder is placed a capillary tube (1.5 mm of internal diameter) which purges the carrier gas (He).

Thus, the toluene-saturated helium enters the cooler (**Figure 2.1.2.1 - b**) set at 4.5°C to reach the exact concentration according to the Antoine law. The cooler is made of two concentric tubes (6mm and 12mm of internal diameter): in the internal tube flows the toluene-saturated helium, while in the external one the coolant liquid.
The two parts are linked to each other thanks to a rotulex 13/5 junction.

2.1.3 Reactor cell

As mentioned before, one of the main objectives in the *operando* methodology is the possibility of in situ characterization combined with the online analysis of products under actual reaction conditions. Therefore, using just an ordinary in situ reactors or reactor cells cannot fulfil the purpose. In fact, in situ reactors for *operando* investigations should simulate as similar as possible realistic reaction conditions to obtain meaningful information. For this reason, plug flow reactors are preferred for this methodology rather than batch reactors, which also could alter the catalytic events due to the possibility of readsorption of reaction intermediates that can happen in this kind of reactors.
Further features should be also considered in the design of an *operando* reactor cell: low dead volume, good reactant-catalyst contact during the reaction, variable space velocity and a uniform as possible temperature profile to conduct isothermal experiments.
To achieve all these characteristics, a homemade reactor is employed in this work. It consists on a sandwich IR cell reactor, which is a widely used kind of reactor cell for *Operando* IR investigations at laboratory scale. An illustrative example of the reactor scheme representation is reported in **Figure 2.1.3.1**.

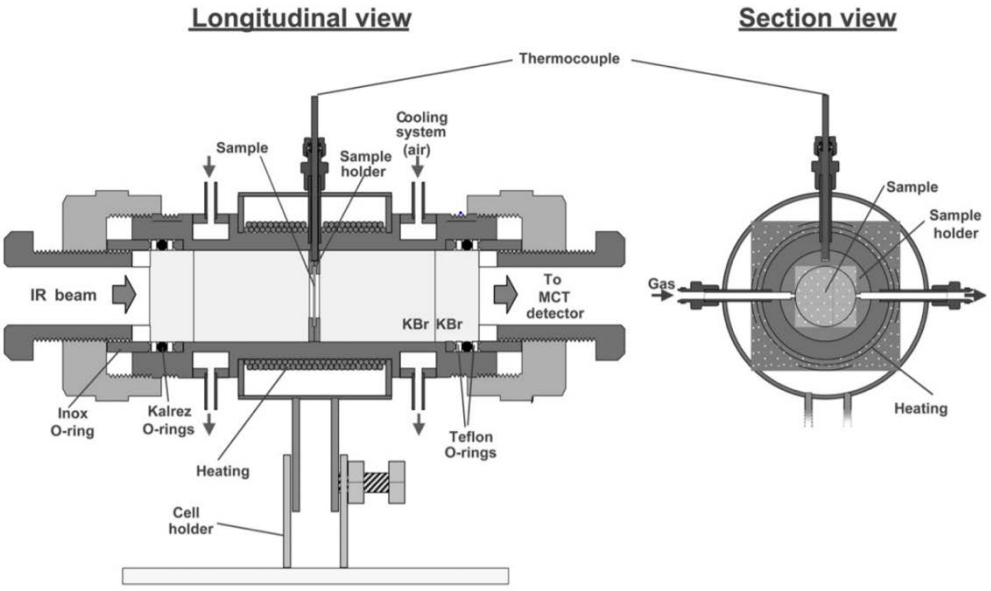

Figure 2.1.3.1 *Illustrative example scheme of the reactor cell design [47].*

The reactor consists of a stainless-steel cylinder supporting a circular sample holder in the middle, where the catalyst is placed as a self-supported wafer. The system is then placed inside an oven which controls the temperature on the sample during the experiments and also maintains the system at isothermal conditions. The remaining space in the cylinder is filled with KBr windows (three for each side) transparent to the IR beam to limit the dead volume in the cell.

The sample holder is also homemade and specifically designed to keep the catalyst wafer in position in the reactor cell (**Figure 2.1.3.2**). It is comprehensive of two symmetrical discs (25mm of diameter) to keep the catalyst on vertical position, it is also engineered with six capillary channels (200 μm of internal diameter) to provide a uniform distribution of the inlet gas on the

wafer, the same configuration is employed for the outlet and a dedicated hole for the thermocouple is located on top. Both the discs present a circular hole (9 mm of diameter) in the center to let that portion available for the IR analysis. The volume of the cell without the catalyst in its position is 283 mm^3, while the effective volume occupied by the gas in the is 276 mm^3 due to the presence of the wafer.

Thus, the cell is connected to the flow lines and to the analysis instrumentations.

In **Figure 2.1.3.3** an overview of the reactor connected to the system is reported.

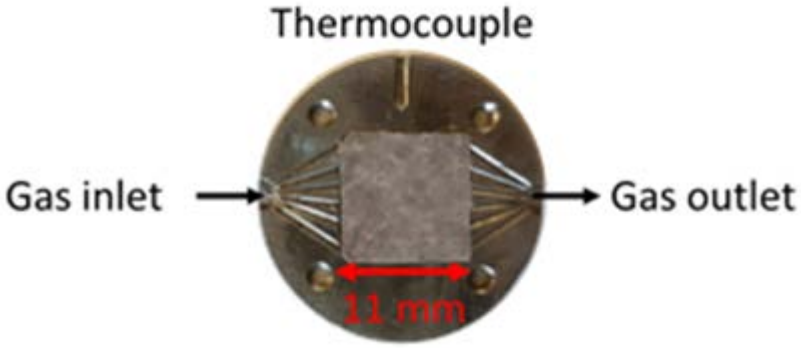

Figure 2.1.3.2 *Sample holder used in the reactor cell with the catalyst wafer in position.*

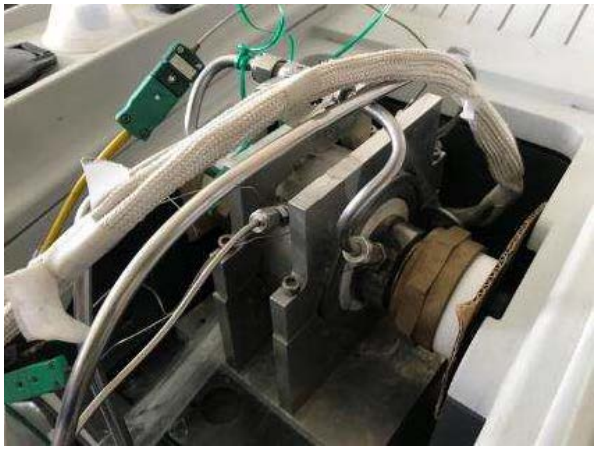

Figure 2.1.3.3 *Reactor cell loaded in the FTIR.*

2.2 Analysis Instruments

In this section the analysis instruments implemented for the *Operando* study are descripted. In particular, a FT-IR spectrometer, a mass spectrometer and a micro-gas chromatographer are used simultaneously to provide a surface and gas phase analysis under actual reaction conditions.

2.2.1 FT-IR Spectrometer: Thermo Scientific Nicolet 380

A *Fourier-transform infrared* spectrometer is the predominant analysis instrument for the acquisition of infrared spectra of solids, liquids or gas because it is able to simultaneously collects high-spectral-resolution data over a wide spectral wavenumber range. This represent a significant improvement if compared with the previous *dispersive* spectrometers which limit was the narrow wavenumber range of the measurement.
The idea behind Fourier-transform infrared spectrometry is that the interference of radiation between two beams provides an *interferogram*, which is a signal generated by changing the pathlength between two beams. Then, a Fourier transform converts the interferogram into an actual spectrum. In **Figure 2.2.1.1** a schematic representation of the basic components of a FT-IR spectrometer is reported.

Figure 2.2.1.1 *Components of a FT-IR spectrometer.*

The radiation, coming from the source, passes through the interferometer and the sample to reach the detector. Once the signal has been amplified, the analog data are converted into digital ones thanks to an analog-to-digital converter and sent to a computer for the Fourier transformation.
In this work, the IR spectra obtained by the transmission technique are used to investigate in situ the evolution of the adsorbed species on the catalyst during the on-going reaction. They are collected by a *Thermo Scientific Nicolet 380* FT-IR spectrometer (**Figure 2.2.1.2**) placed perpendicularly to the wafer, equipped with a liquid nitrogen cooled MCT detector. To improve the signal-to-noise ratio, 128 scans at a resolution of 4 cm^{-1} are accumulated to have a spectrum every 2.08 min.
The mercury cadmium telluride (MCT) detector is preferred in this configuration, instead of the more common deuterium triglycine sulfate (DTGS) detector, because of the very low

flowrate of the IR throughput. Moreover, this detector is able to reduce the sampling time without affecting the sensitivity.

Figure 2.2.1.2 *Thermo Scientific Nicolet 380 FT-IR spectrometer.*

Ultimately, the output of the instrument is a series of spectra in the mid-infrared region (4000 – 400 cm^{-1}) where the ordinate scale is the absorbance.

2.2.2 Quadrupole Mass Spectrometer: Pfeiffer QMS 200

A quadrupole mass spectrometer (QMS), also quadrupole mass filter or quadrupole mass analyser, is a widely used instrument for the analysis of residual gas compositions through the measure of the mass-to-charge ratio (m/z) of ionized atoms.

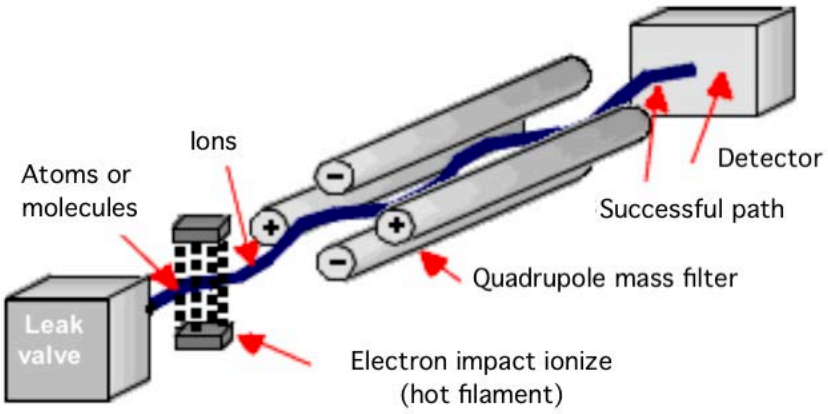

Figure 2.2.2.1 *Schematic representation of principle of working of a QMS.*

A QMS is composed by three main parts: an ionizer, an ion accelerator and a quadrupole (mass filter) which consists of four cylindrical parallel rods arranged in a square where the opposite ones are electrically paired with a positive or a negative charge. The general principle of working of the QMS is represented in ***Figure 2.2.2.1***.
Electrons from a hot filament bombards the gas flow to analyze causing the molecules fragmentation into ions. Now the ions enter the quadrupole where they are affected by a fixed and an oscillatory electric field, which affect them trajectory resulting in a sinusoidal deviation. Thus, only certain ions are able to reach the detector, an electronic transducer able to amplify the current produced by the ions, located at the end of the quadrupole. The produced signal is then converted by a computer software in a "stick diagram" where for each mass-to-charge ratio is shown the relative current produced by the ions.

Figure 2.2.2.2 *Pfeifer QMS 200.*

In this study, the MS data are used for analyzing the actual reaction products and they are collected with a *Pfeiffer QMS 200* (**Figure 2.2.2.2**)with a time-resolution of 3.2 s. In **Table *2.2.2.1*** the analyzed mass-to-charge ratio are reported.

Table 2.2.2.1 *Mass-to-charge ratio considered in the study.*

Scanned m/z	Corresponding Gas
4	He
18	H_2O
28	CO
32	O_2
43	Butane
44	CO_2
68	Furan
78	Benzene
84	Cyclohexane
91	Toluene
106	Benzaldehyde
108	Benzoquinone
122	Benzoic acid

2.2.3 Gas Chromatograph: Aligent 490 Micro-GC

The gas chromatograph (GC) is widely used analysis instrument for the analysis of mixtures composition. It is able to separate compounds that can be vaporized without decomposition thanks to a chromatograph column and then analyze them thanks to a detector placed in series with the column.

For this study, an *Aligent 490* micro-GC (***Figure 2.2.3.1***) equipped with a TCD detector is employed to monitor O_2, CO and CO_2 in the reaction products during the experiments with a time-resolution of 5 min. (Moreover, it helps to understand whether there are leaks in the system.

Figure 2.2.3.1 *Aligent 490 micro-GC.*

The thermal conductivity detector (TCD), also known as katharometer, is a widespread detector which records changes in thermal conductivity of the gas coming from the chromatograph column. In particular, to a change in the gas composition corresponds a change in the thermal conductivity which is recorded by the computer.

2.3 Experimental procedures

In this paragraph the model reaction used to test the system will be introduced, the procedure for the preparation of the catalysts described and the operation conditions illustrated.

2.3.1 Catalyst preparations

All the experiments are carried out on 1%wt Pt/γ-Al_2O_3 catalyst in two different platinum oxidation states: an oxidase state of Pt (δ+) and a reduced state of Pt (0) obtained with two different in situ treatments that will be described later on.

The 1%wt Pt/γ-Al_2O_3 catalyst is provided by IFPEN (IFP Energies Nouvelles) and prepared through wet impregnation technique by the providing company as follow [55]:

1. γ-Al_2O_3 is mixed for flew hours with a solution of chloroplatinic acid (H_2PtCl_6), which concentration is adjusted to obtain 1%wt Pt;
2. The solution is calcinated at 520°C for 2h with dry air (1 L/g h);
3. The catalyst is dechlorinated at 520°C with a wet air flow (8000 ppm/h of water);
4. Finally, the catalyst is reduced at 500°C for 2h under H_2 flow (1 L/g h).

At the end of the preparation, the catalyst takes the form of a granular sand, whose features given by IFPEN are reported in **Table *2.3.1.1***.

Table 2.3.1.1 *Catalyst specifications by IFPEN.*

Specific surface	189 m^2/g
Pt dispersion	74%
Avr. diameter of Pt particles	1.4 nm

Now, the catalyst grains are crashed into a thin powder (***Figure 2.3.1.1-a***) and pressed under 100 MPa to obtain a leaf of about 100 μm of thickness, which is shaped in a square wafer of 1.21 cm^2 (1.1cm x 1.1cm) for *Operando* IR investigations (***Figure 2.3.1.1-b***). Then the sample is put in the right position in the sample holder (***Figure 2.3.1.1-c***), loaded in the reactor cell and connected to the *Operando* set-up.

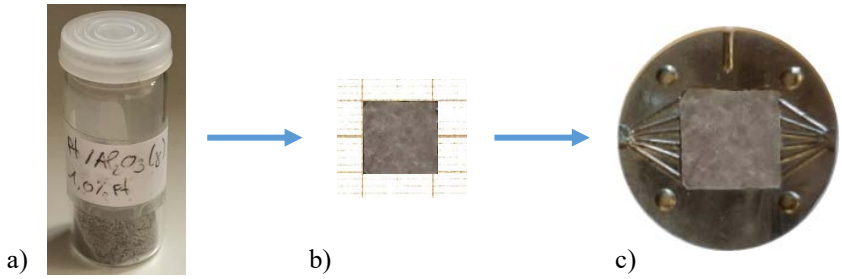

a) b) c)

Figure 2.3.1.1 *a) powder of Pt/γ-Al_2O_3 b) shaped wafer c) catalyst sample in the sample holder.*

Once loaded and connected, two different in situ thermic pre-treatments are performed on the catalyst: to obtain the oxidize Pt, a mixture of 10% of O_2 in Ar at 350°C is sent on the sample for 4h; while for the reduced Pt, a mixture of 5% of H_2 in Ar at 400°C for 4h.
Additionally, a third catalyst condition is tested, i.e. a 1%wt Pt/γ-Al_2O_3 catalyst where the average Pt particle diameter is 20nm, simulating their sintering. The preparation of the wafer reported above also applies for this catalyst and only the Pt oxidize state pre-treatment is performed.
Lastly, consideration on the weight of the catalyst should be made in order to work in reaction conditions as similar as possible to real ones and consequently obtain reliable data. Whit this in mind, the catalyst mass/reactant amount ratio (w/F) is calculated and kept as low as possible. The average values obtained for the catalysts with 1.4nm and 20nm Pt particles are showed in **Table *2.3.1.2***.

Table 2.3.1.2 *Catalyst weight-reactant amount ratio for the employed catalysts.*

Catalyst	**w/F [g s/cm^3]**
Pt 1.4nm	0.016
Pt 20nm	0.021

Thus, the catalyst weight is adapted to obtain w/F values which well fit the ones of automotive exhaust catalysts [47].

2.3.2 Flowrate composition and operating conditions

All the experiments are carried out in order to have a toluene concentration of 800ppm in 10%vol O_2 and He (inert) as reagent gas mixture (***Figure 2.3.2.1***).

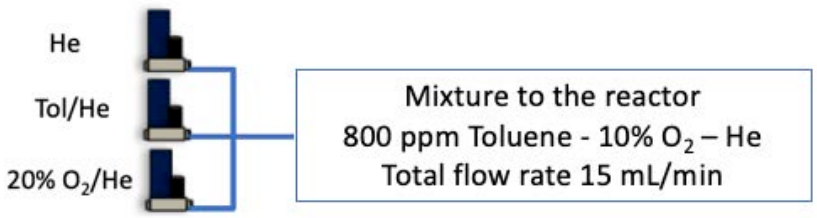

Figure 2.3.2.1 *Schematic representation of the mixture to the reactor.*

The composition of the reaction mixture is reported in **Table *2.3.2.1***.

Table 2.3.2.1 *Composition of the reaction mixture to the reactor cell.*

Component	Toluene	O_2	He
%	0.08	10	89.98

Concerning the operating conditions, all the tests are performed at ambient pressure with a temperature profile studied to evaluate the catalyst activity: ramp up and ramp down. In fact, temperature ramping tests make it possible to assess the dynamic response of the reactant mixture and, since the evolution of the species adsorbed on the catalyst is also investigates, allow to understand which intermediates species are present at different temperatures.
In the set-up the temperature is automatically controlled by a computer interface which set the temperature of the oven where is located the reactor cell. Both in temperature increasing and in decreasing, it is applied a ramp of 3°C/min from 50°C to 450°C and vice versa (**Figure 2.3.2.2**).

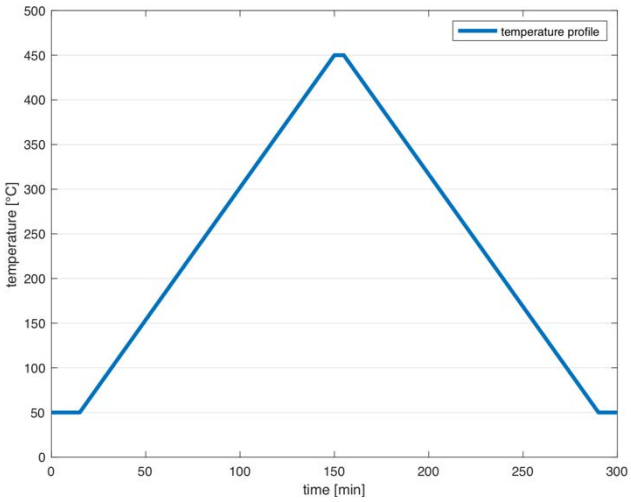

Figure 2.3.2.2 *Temperature profile set in the oven.*

Considering these operating conditions, the thermocouple located in the sample order detect a maximum temperature of 400°C.

Chapter 3

Results and Discussion

3.1 Catalytic performance studies

The catalytic activity of the catalysts investigated towards toluene oxidation is evaluated through the calculation of toluene conversion and CO_2 yield as a function of temperature.

3.1.1 Conversion and Yield calculations

The experimental data coming from the MS are processed with MATLAB® in order to quantify the variation in composition of reactants and products.
Since the reaction occurs with an increasing of the number of moles, the total flowrate increases with the progress of the reaction. Thus, if the conversion of the i^{th} specie is calculated as in Eq. 3.1, where y_i is the molar fraction and $\dot{N}$ the total molar flowrate, the inlet molar fraction, the total inlet flowrate and the outlet molar fraction are known. Indeed, the outlet total flowrate is unknown. Thus, Eq. 3.1 cannot be used for the conversion estimation.

$$X_i = \left(1 - \frac{y_i^{out}\dot{N}^{out}}{y_i^{out}\dot{N}^{out}}\right) \cdot 100 = \left(1 - \frac{\dot{n}_i^{out}}{\dot{n}_i^{out}}\right) \tag{3.1}$$

However, a correlation is implemented in MATLAB®, which is able to calculate the ppm of toluene exiting the reactor knowing the intensity of the corresponding signal (m/z=91) in the MS. As a consequence, the conversion of toluene is calculated through the experimental data as Eq. 3.2, where ppm_{Tol}^{in} represents the amount of toluene in the inlet feed gas, whereas ppm_{Tol}^{out} is the amount of toluene in the effluent gas.

$$X_{Tol} = 1 - \frac{ppm_{\mathrm{Tol}}^{out}}{ppm_{Tol}^{in}} \tag{3.2}$$

T_{50} and T_{90} parameters are introduced to evaluate the evolution of the catalytic activity and they represents the temperature at which toluene conversion is 50% and 90%, respectively.
The yield is defined as the ratio between the amount of CO_2 produced over the amount of Toluene entering the reactor in terms of ppm as reported in Eq. 3.3. The ppm of CO_2 are obtained, as for toluene, through a correlation from the experimental intensities of the related mass-to-charge ratio (m/z=44).

$$Y_{CO_2/Tol} = \frac{1}{7} \cdot \frac{ppm_{CO_2}^{out}}{ppm_{Tol}^{in}} \tag{3.3}$$

Defined in this way, the yield is equal to 100% when all the toluene entering the reactor is converted in CO_2.

3.1.2 Toluene Conversion

The toluene conversions curves as a function of temperature over $fPt^{\delta+}/\gamma\text{-}Al_2O_3$, $fPt^0/\gamma\text{-}Al_2O_3$ and $aPt^{\delta+}/\gamma\text{-}Al_2O_3$ are determinate and reported in **Figure 3.1.1**. The measurements are performed at constant inlet composition and total flowrate (800ppm of toluene – 10%O_2 – He, 15 mL/min).
As shown in **Figure 3.1.1**, the conversion curves display the characteristic sigmoidal behavior of hydrocarbon oxidation systems. Among the conditions considered, in general the aged catalyst ($aPt^{\delta+}$) exhibits the lower catalytic performances.
Instead, considering the performance of fresh catalysts with different Pt oxidation state ($Pt^{\delta+}$and Pt^0), it seems that around 190°C there is an inversion of activity:

- below 190°C, Pt in its oxidized state ($Pt^{\delta+}$) is more active compared to the reduced state (Pt^0), also supported by the fact that conversion starts at a lower temperature using the Pt oxidized catalysts;
- above 190°C, Pt in its reduced state (Pt^0) promotes better the reaction and at the end the total conversion is reached at a lower temperature.

On all catalysts, toluene conversions higher than 95% are reached before 300°C.
Comparison of the results indicates also a distinction of activity to make for lower and higher temperatures. In fact, at low temperatures (50°C -175°C) the activity order is: $fPt^0 < aPt^{\delta+} < fPt^{\delta+}$, while at high temperatures (>250°C) the order is different: $fPt^{\delta+} < aPt^{\delta+} < fPt^0$. Thus, $aPt^{\delta+}$ conversion curve lays between the two fresh catalysts which invert their behavior as reported above.

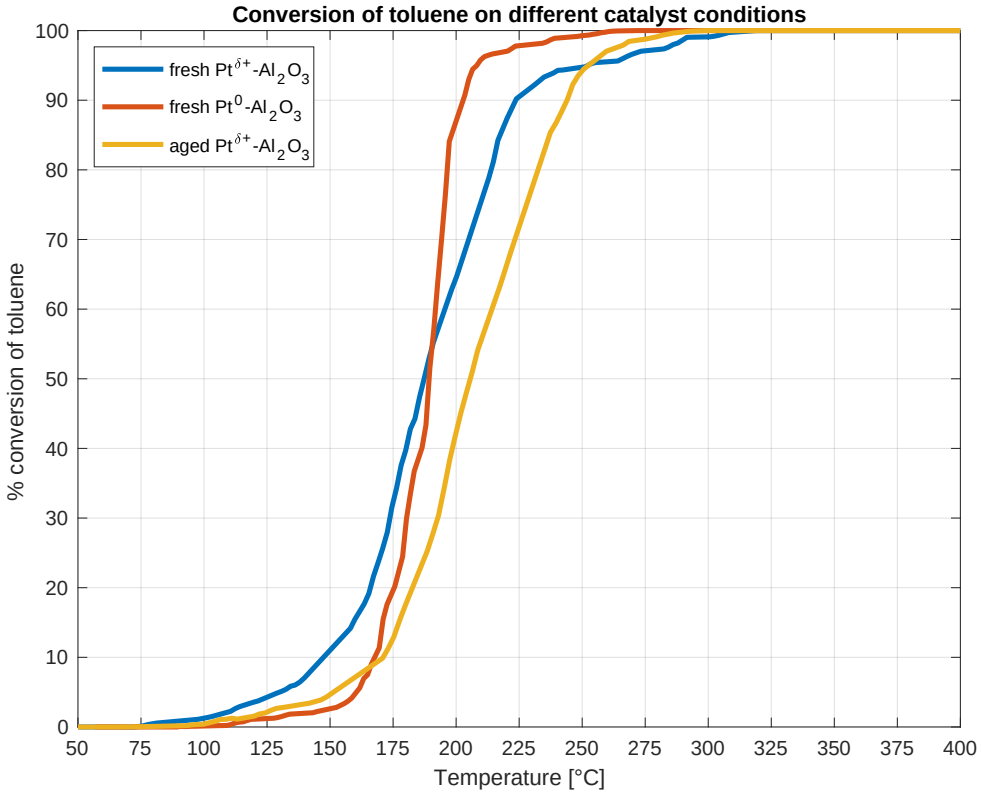

Figure 3.1.1 *Toluene conversion curves as a function of temperature on different catalyst conditions.*

To have a more analytic comparison on the catalytic activities the T_{50} and T_{90} (temperature at which toluene conversion is 50% and 90%, respectively) are estimated and displayed in **Table *3.1.1***. In terms of T_{50}, the following increasing order of activity is obtained: $fPt^{\delta+} \sim fPt^0 < aPt^{\delta+}$.

Table 3.1.1 *T_{50} and T_{90} values for studied catalyst conditions.*

Pt oxidation state	d_{Pt} [nm]	Conversion		Yield	
		T_{50} [°C]	T_{90} [°C]	T_{50} [°C]	T_{90} [°C]
$Pt^{\delta+}$	1.4 (fresh)	187	220	200	269
	20 (aged)	206	245	222	258
Pt^0	1.4 (fresh)	190	200	200	237

The values obtained quite agree with the literature (**Table *1.2.1***), taking into account that the T_{50} depends on the dispersion and the oxidation state of Pt on the surface of the catalyst and on the amount of toluene fed to the reactor [47][48].

To have more insights on the evolution of the reaction, also the yields in CO_2 curves as a function of temperature are determinate for each catalyst condition and reported in **Figure 3.1.2**. The calculations are made on the same experiment of the conversion calculation to have comparable results.
The same comments made for the conversion curves still stand for the yield, but, if the T_{50} parameter is considered (temperature at which toluene yield in CO_2 is 50%), in all the catalysts conditions a shift in it is reported (**Table *3.1.1***). This result can be explained with the presence of reaction intermediates. Further investigations will be provided later on.

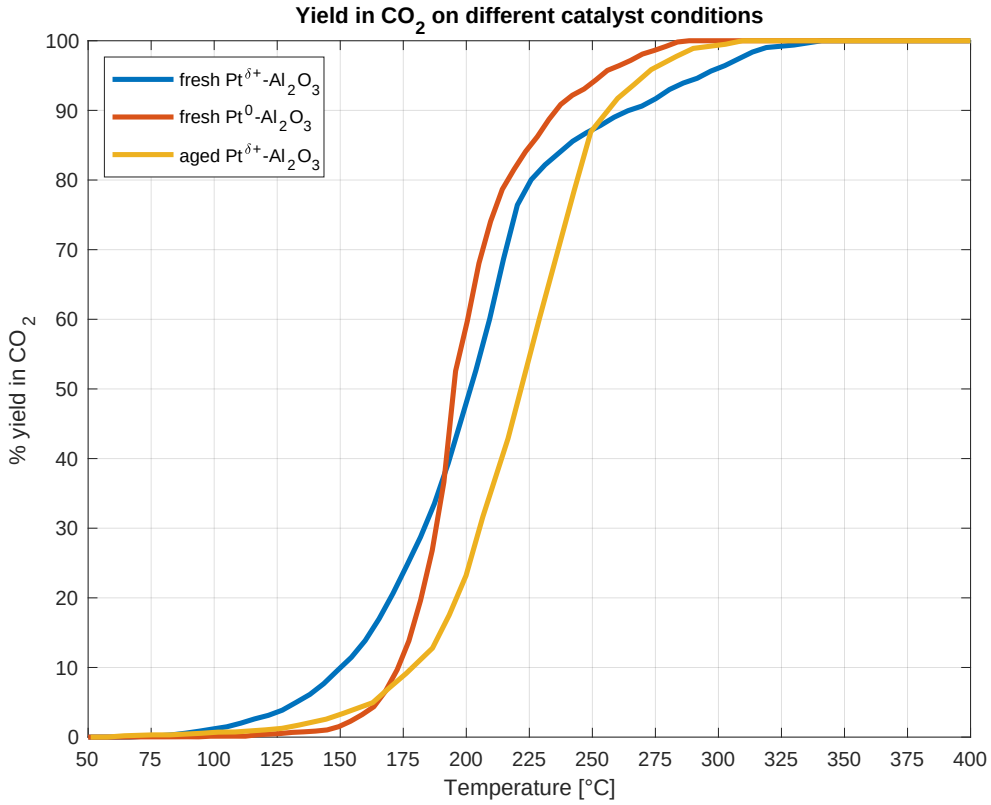

Figure 3.1.2 *Yield into CO_2 as a function of temperature on different catalyst conditions.*

3.2 Investigation of the controlling regime

The experimental data used for the calculation of the conversion curves are used also to investigate the system controlling regime and to have more insights on the intrinsic kinetic of the reaction on different catalyst conditions, presented in Section 2.3.1.

3.2.1 Mathematical Model

In order to better understand the reaction mechanism and the controlling regime, a mathematical model of the system is proposed.

The reactor described in Section 2.1.3 is modelled as a PFR without temperature gradients inside the catalyst. Since, the reactor is fed with a constant flowrate and the gas volume changes with temperature, also the residence time changes inside the reactor. In particular, an increase of temperature causes a decrease in the residence time. As the temperature rise is low (3°C/min) compared to the residence time (1–5s), the reactor can be assumed to be isothermal at each time in the simulation.

The system is also modelled as comprehensive of a gas and a solid phase: the former represents the mixture entering the system, while the latter the catalyst. In particular the solid phase is assumed not permeable, so the reaction occurs only on the catalyst surface.

Under these assumptions, the isothermal mass balances to solve, for both toluene and O_2, in order to obtain the calculated concentrations are reported in Eq. 3.4 for the gas phases and Eq. 3.5 for the solid phase.

$$MB_i^G \qquad \frac{dc_i^{G,b}}{d\tau} = -h_{m,i}^G (c_i^{G,b} - c_i^{G,i}) \cdot a^G \tag{3.4}$$

$$MB_i^S \qquad 0 = r''^S_i + h_{m,i}^G (c_i^{G,b} - c_i^{G,i}) \tag{3.5}$$

In these equations τ [s] is the residence time, $h_{m,i}^G$ [m/s] is the effective mass transfer coefficient and a^G [1/m] is the specific area of the catalyst, which is calculated as in Eq. 3.6, where A^{GS} [m^2] is the active surface of the catalyst (two times the surface area of the wafer) and V^G [m^3] the volume occupied by the gas phase in the reactor.

$$a^G = \frac{A^{GS}}{V^G} = \frac{2 * l^2}{Vol_{Empty} - Vol_{Cat}} \tag{3.6}$$

The effective mass transfer coefficient of the ith specie $h_{m,i}^{G}$ is obtained rearranging the definition of the Sherwood number *Sh* reported in Eq. 3.7, where D_i is the diffusion coefficient of the ith specie and L the reactor cell length.

$$Sh = \frac{L \cdot h_{m,i}^{G}}{D_i} \tag{3.7}$$

The Sherwood number is given by the correlation reported in Eq. 3.8 [56], where *Re* is the Reynolds number and *Sc* the Schmidt number, defined as Eq. 3.9-10 [56].

Sherwood number $$Sh_L = 0.66 \cdot Re_L^{1/2} Sc^{1/3} \tag{3.8}$$

Schmidt number $$Sc = \frac{v\rho L}{\mu} \tag{3.9}$$

Reynolds number $$Re_L = \frac{v\rho L}{\mu} \tag{3.10}$$

Lastly, r''^{S}_{i} [mole/(s m^2)] is the production rate of the ith specie, which is both function of the gas interface concentrations and the solid concentrations ($r''^{S}_{i} = f(c_i^{G,i}, c_i^{S})$). The two concentrations are related thanks to the assumption of adsorption equilibrium, which links them with a proportional law. It assumes that at the interface there is local equilibrium. Thus, r''^{S}_{i} is given by Eq. 3.11, where ν_i is the stochiometric coefficient and R'' is the intrinsic reaction rate.

$$r''^{S}_{i} = \nu_i \cdot R'' \tag{3.11}$$

The formulation of the reaction rate R'' is given by two contribution, one depending on temperature and the other on reactant concentrations. The temperature dependency follows the Arrhenius law (Eq. 3.12).

$$k''(T) = A \cdot \exp\left(\frac{-E_a}{RT}\right) \tag{3.12}$$

A [1/s] is the pre-exponential factor, E_a [J/mole] the activation energy, R [J/(mole K)] the gas constant and T [K] the temperature.
The concentration depending term, instead, changes according to the kinetic model.
A literature review [42][57] shows that the toluene oxidation can be approximated by a first order kinetics, corresponding to a zero-order dependency in oxygen concentration and first-order dependency in toluene concentration. Thus, the reaction rate is expressed by Eq. 3.13.

$$R'' = k'' \cdot c_{Tol} \tag{3.13}$$

The pre-exponential factor A and the apparent activation energy E_a are determinate from the experimental results. The algorithm implemented through the script solves the mass balances (Eq. 3.4 – 3.5) and calculates the theoretical concentrations (c_i^{calc}) and compares them to the experimental ones, obtained from the temperature ramping tests (c_i^{exp}), through the defined objective function (Eq. 3.14).

$$F_{obj} = \left\| c_i^{calc} - c_i^{exp} \right\|_2 \tag{3.14}$$

Thus, in order to optimize the mathematical model, the algorithm varies the A and E_a values for minimizing the objective function.
In **Figure 3.2.1.1** a schematic flow chart of the algorithm is represented.

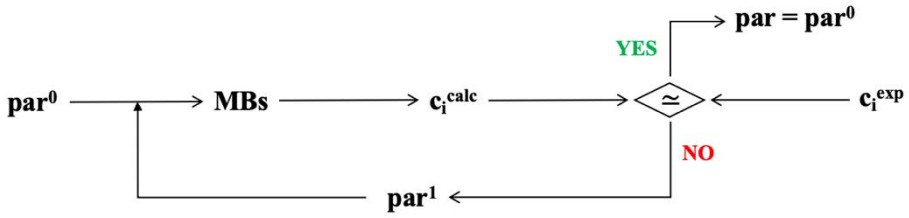

Figure 3.2.1.1 *schematic flow chart of the MATLAB® script.*

To have insights on which mechanism, between kinetics and mass transfer, is controlling the reaction, three different conditions are simulated:

1. single phase PFR under kinetic control only;
2. pseudo-1D PFR under mass transfer control.

3.2.2 Kinetic control regime

Under kinetic control regime, mass transfer is assumed much faster compared to the kinetics, so that the gas concentration in the bulk can be assumed equal to the gas concentration on the interface. Consequentially, the contribution $\left(c_i^{G,b} - c_i^{G,i}\right)$ in Eq. 3.4 – 3.5 tends to zero, making possible to rearrange the mass balances and obtain only two ordinary differential equations (Eq. 3.15), one for toluene and one for O_2, to solve with the MATLAB® script.

$$\begin{cases} \dfrac{dc_{tol}^{G,b}}{d\tau} = A \cdot \exp\left(\dfrac{-E_a}{RT}\right) \cdot c_{Tol} \cdot a^G \\ \dfrac{dc_{O_2}^{G,b}}{d\tau} = 9 \cdot A \cdot \exp\left(\dfrac{-E_a}{RT}\right) \cdot c_{Tol} \cdot a^G \end{cases} \tag{3.15}$$

Thus, the above mathematical model is applied to fit the experimental data obtained from the toluene oxidation over each catalyst and the results are given as comparison of the experimental versus calculated concentrations in **Figure 3.2.2.1**, while the estimate values the apparent activation energy are listed in **Table 3.2.2.1**.

Table 3.2.2.1 *Estimated values of the pre-exponential factor A and apparent activation energy E_a for each catalyst condition.*

	***A* [1/s]**	***E_a* [kJ/mole]**
$fPt^{\delta+}$	19.9	15.2
fPt^0	103	17.7
$aPt^{\delta+}$	90.9	19.3

As shown in **Figure 3.2.2.1**, the experimental data are well fitted by the proposed mathematical model in all the considered cases, thus it can be assumed that the system is under kinetic control and the toluene oxidation can be approximated with a first order kinetics referred to toluene concentration and zero oxygen order (Eq. 3.13).

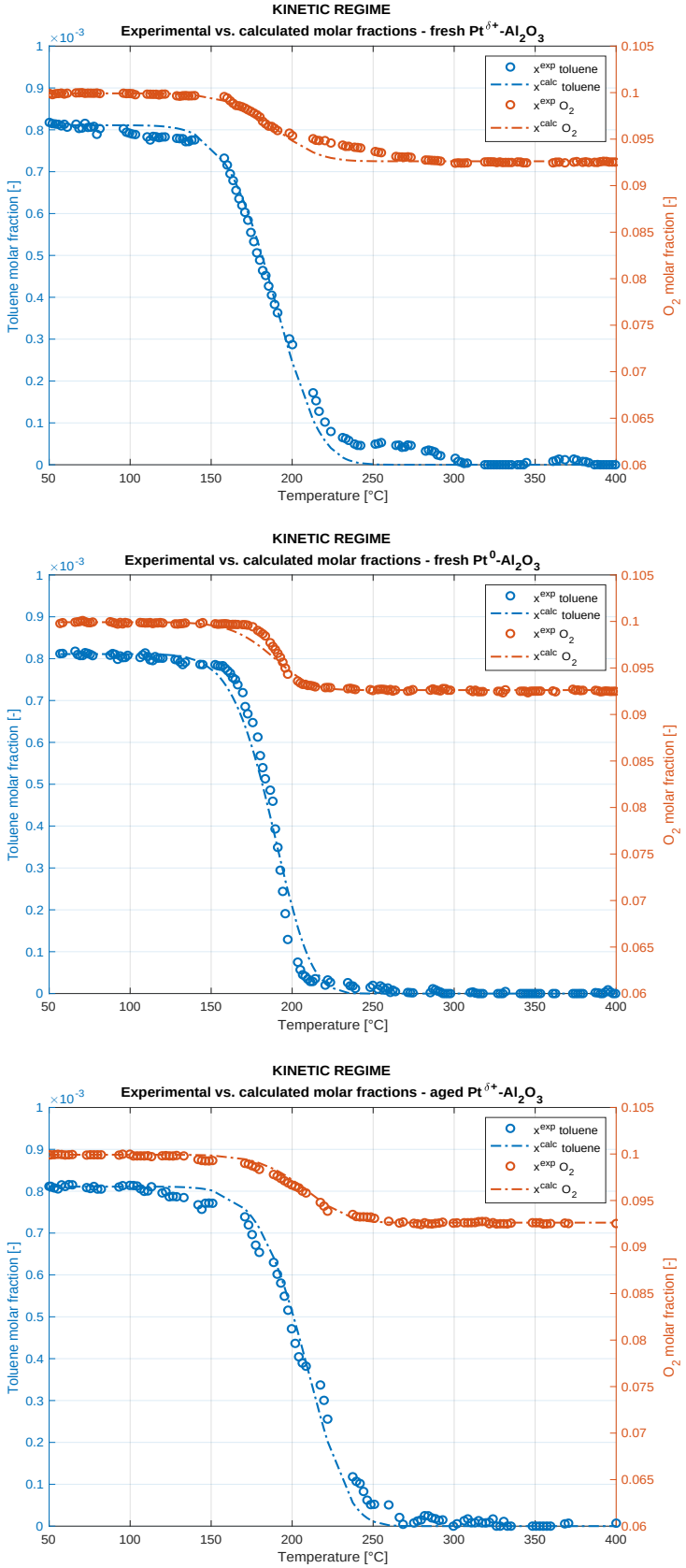

Figure 3.2.2.1 *Comparison between experimental molar fractions and the values calculated by the model under kinetic control over a) fPt$^{\delta+}$/γ-Al$_2$O$_3$, b) fPt^{0}/γ-Al$_2$O$_3$ and c) aPt$^{\delta+}$/γ-Al$_2$O$_3$ catalysts.*

3.2.3 Mass Transfer control regime

Under mass transfer regime, kinetics is assumed much faster compared to the mass transfer, so that each reactant molecule which comes near the catalyst surface is immediately consumed, meaning $c_i^{G,i}$ tends to zero. Thanks to this assumption, the kinetic information disappears from the mass balances which becomes Eq. 3.16. The kinetic parameters are not needed, so the optimization is unnecessary in these conditions.

$$\frac{dc_i^{G,b}}{d\tau} = -h_{m,i}^{G} \cdot c_i^{G,b} \cdot a^{G} \tag{3.16}$$

Therefore, we have just to solve two algebraic equations (Eq. 3.17), one for toluene and one for O_2, to calculate the exiting concentrations.

$$\begin{cases} c_{tol}^{G,b}(\tau) = c_{tol}^{G,b}(0)\exp(-h_{m,\mathrm{tol}}^{G} \cdot a^{G} \cdot \tau) \\ c_{O_2}^{G,b}(\tau) = c_{O_2}^{G,b}(0)\exp(-h_{m,\mathrm{O_2}}^{G} \cdot a^{G} \cdot \tau) \end{cases} \tag{3.17}$$

The mathematical model above is applied to fit the experimental data obtained from the toluene oxidation over each catalyst condition and the results are given as comparison of the experimental versus calculated concentrations in **Errore. L'origine riferimento non è stata trovata.**.

Under mass transfer control, the concentrations calculated by the model are underestimated in all the cases considered: calculated concentrations of toluene and O_2 tend to 0.

Therefore, it can be concluded that the mass transfer is not controlling the system. The assumption made in Section 3.2.2 is confirmed, i.e. the system is under kinetic control.

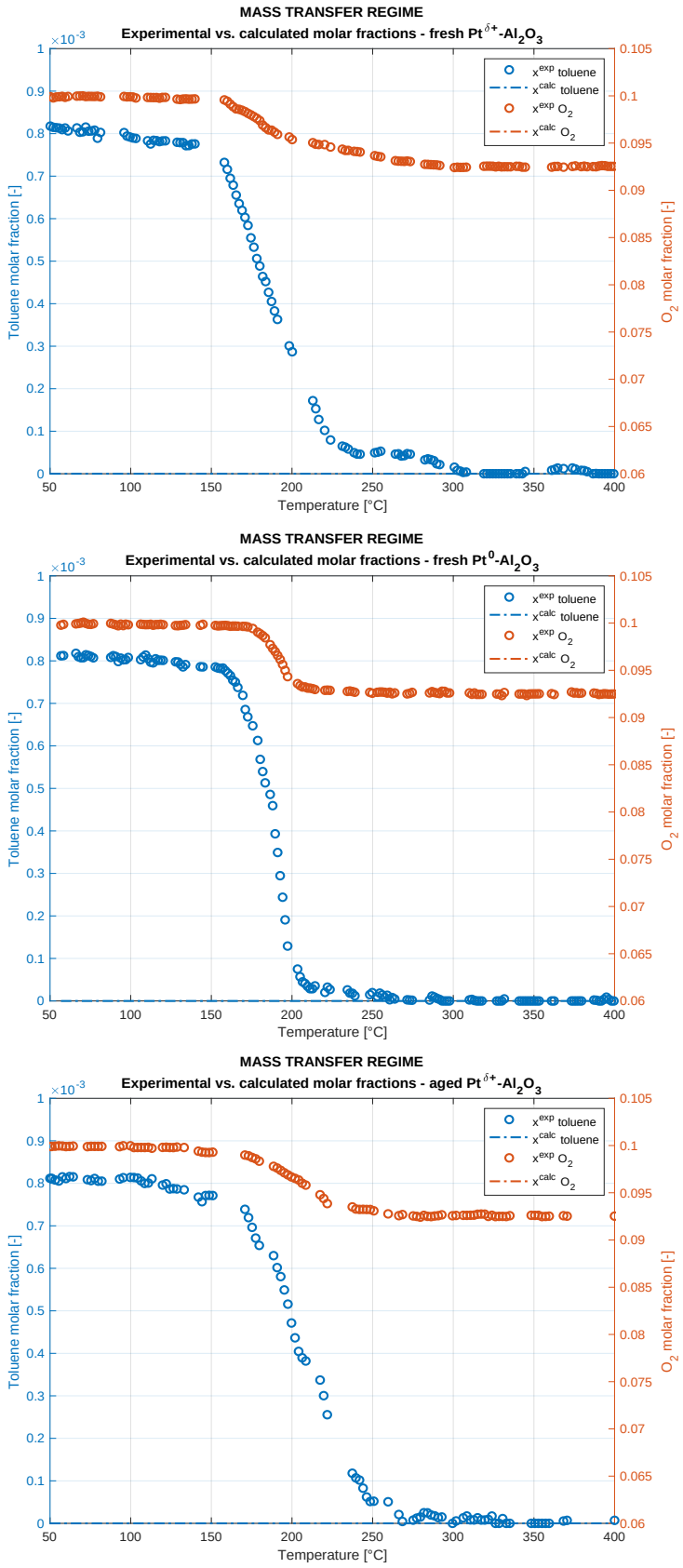

Figure 3.2.3.1 *Comparison between experimental concentrations and the values calculated by the model under mass transfer control over a) fPt$^{\delta+}$/γ-Al$_2$O$_3$, b) fPt^{0}/γ-Al$_2$O$_3$ and c) aPt$^{\delta+}$/γ-Al$_2$O$_3$ catalysts*

3.3 FT-IR spectra investigation

The data obtained from the FT-IR firstly are treated by the Nicolet OMNIC® software and then processed with MATLAB® to perform a deeper analysis.

3.3.1 Reprocessing of the collected data

As mentioned in Section 2.2.1, *in situ* FT-IR spectrometric technique in transmittance mode is adopted to study the model reaction over a Pt-based catalyst in different conditions with respect to the evolution of adsorbed species on the catalytic surface. For the investigation, the Nicolet OMNIC software® is used to collect time-resolved interferograms and to treat them to obtain the relative spectra.

Before the experiment begun, a background interferometer of the system is collected, it is taken with the catalyst wafer loaded in the reactor cell and before the reactant mixture is purged to the system.

Once the background is obtained, the flux to the reactor is switched from only He to the reactant mixture and the experiment can start together with the acquisition of the experimental data. Collecting the background is fundamental because the time-resolved interferometers contain both the information related to the experiment and to the system. Thus, using the background to reprocess the data allows to obtain spectra independent from the initial state of the system and have more insights on the evolution of the reaction.

The reprocess is also needed to convert the interferometers in wavenumber versus absorbance spectra.

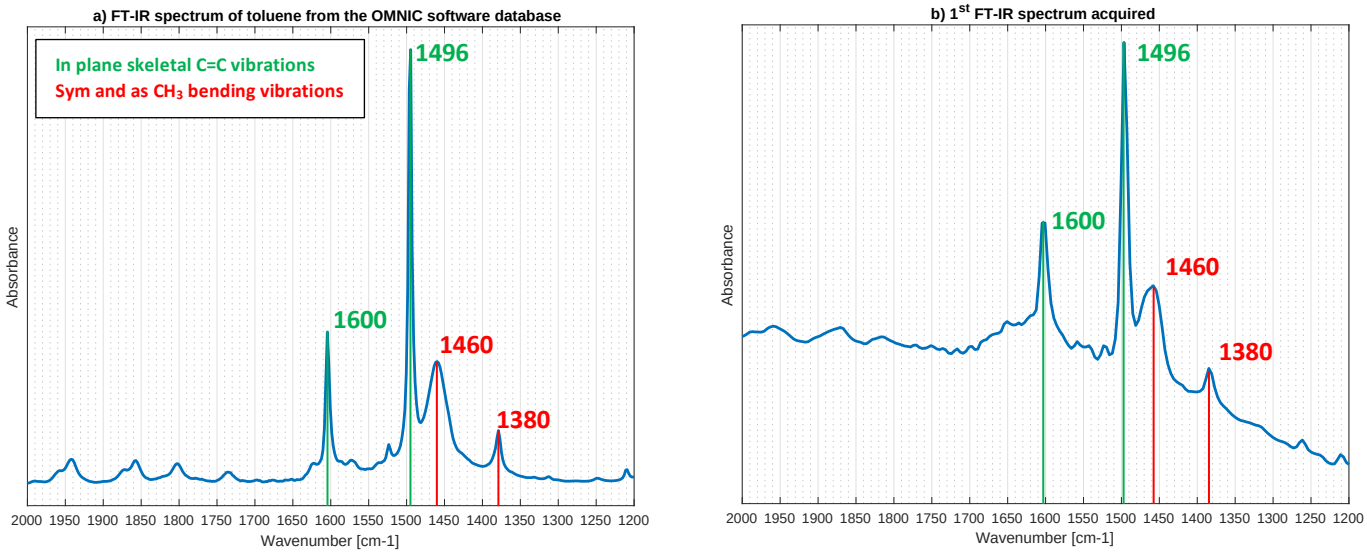

Figure 3.3.1.1 *a) FT-IR toluene spectrum taken from the OMNIC software® database and b) first FT-IR spectrum acquired at X=0for the oxidation of toluene over the fPt$^{\delta+}$/γ-Al$_2$O$_3$ catalyst.*

Figure 3.3.1.1 shows a comparison between the 1st acquired FT-IR spectrum for the test with the fresh $Pt^{\delta+}$ catalyst, at X=0, (**Figure 3.3.1.1-*b***) and the characteristic FT-IR spectrum of toluene present in the OMNIC software® database (**Figure 3.3.1.1-*a***). It can be seen that the spectra are similar to each other and the main toluene peaks can be detected in **Figure 3.3.1.1-*b***.

The bands at 1600 and 1496 cm^{-1} are assigned to the in-plane skeletal vibrations of aromatic ring and bands at 1460 and 1380 cm^{-1} are linked to the asymmetric and symmetric CH_3 bending vibration, respectively [58].

Moreover, for all the experiments, the 1st acquired FT-IR spectrum can be considered as before the reaction on the surface occurs. Thus, for clarity, it is subtracted to all the experiment spectra.

3.3.2 Spectra interpretation

3.3.2.1 Fresh $Pt^{\delta+}/\gamma$-Al_2O_3

The dynamic changes taking place on fresh $Pt^{\delta+}/\gamma$-Al_2O_3 catalyst surface due to the toluene oxidation are monitored through *in situ* transmittance FT-IR spectroscopy and the resulted spectra are reported below.

The wavenumber range of major interest to investigate the evolution of the adsorbed species on the catalyst is between 1900–1300 cm^{-1}, also known as carbonate region.

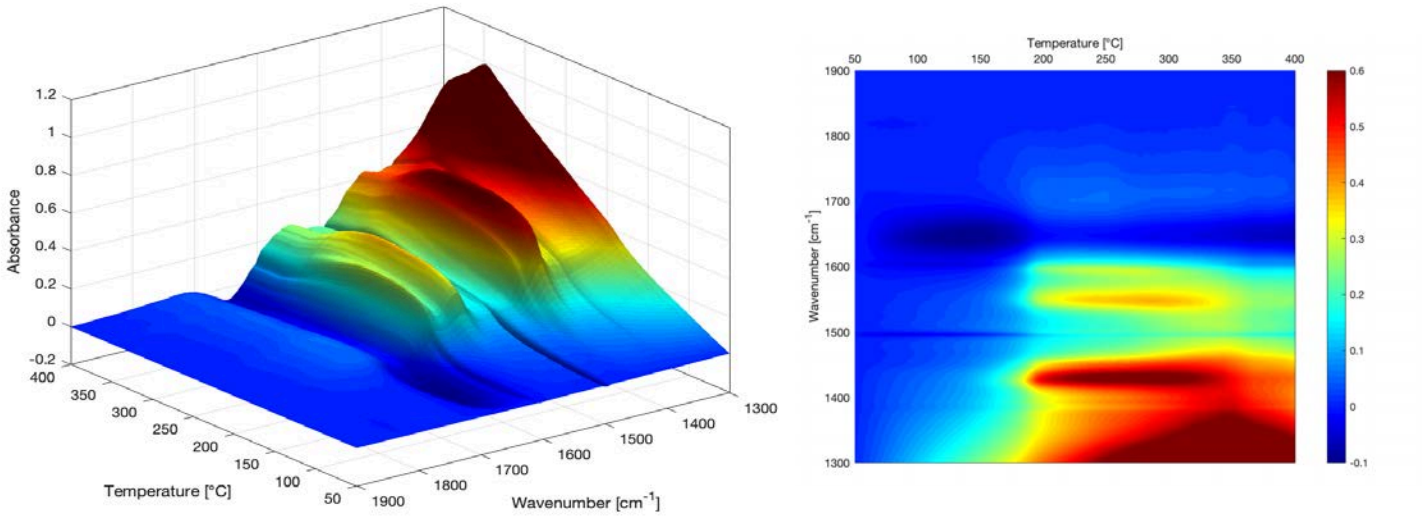

Figure 3.3.2.1.1 *Dynamic changes of the FT-IR spectra in the carbonate region with temperatures over fresh $Pt^{\delta+}/\gamma$-Al_2O_3.*

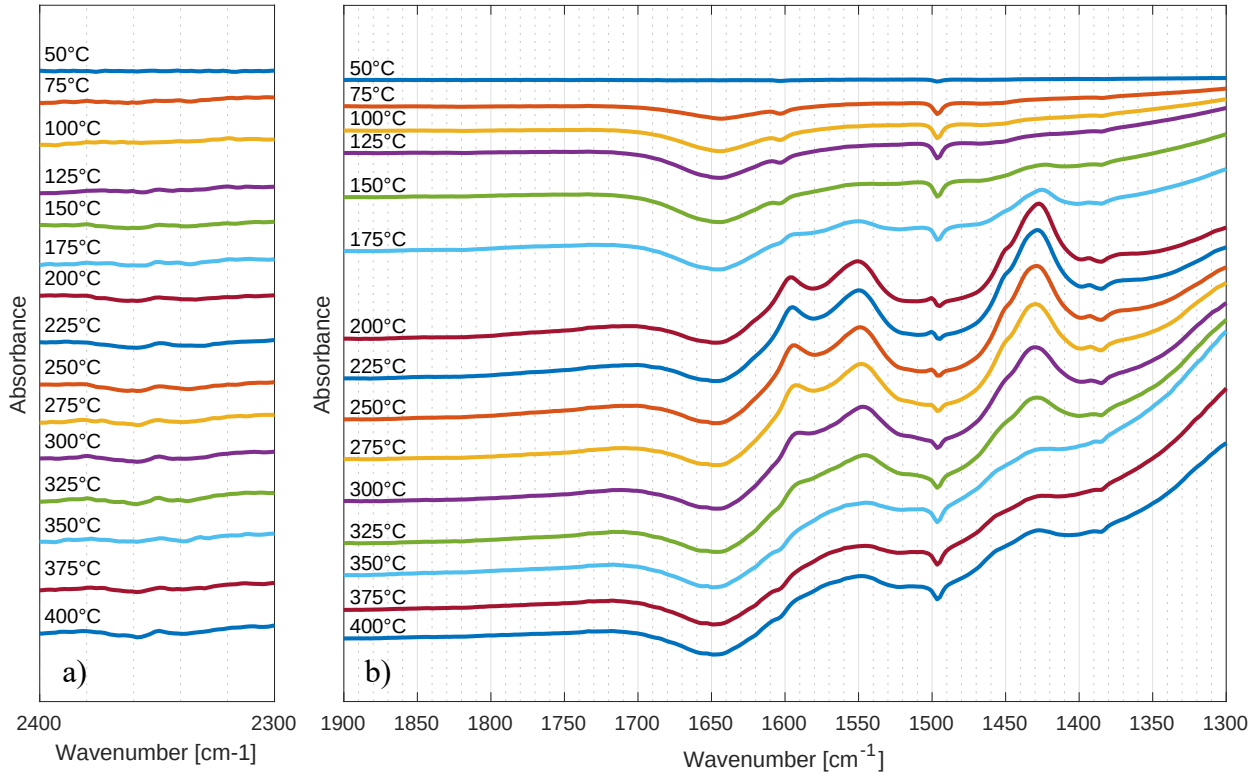

Figure 3.3.2.1.2 *FT-IR spectra each 25°C over fresh $Pt^{\delta+}/\gamma$-Al_2O_3 a) between 2440-2300 cm^{-1} and b) in the carbonate range.*

In **Figure 3.3.2.1.1** and **Figure 3.3.2.1.2-*b*** the evolution in the FT-IR spectra in this range, as a function of temperature, is reported.

At the beginning the negative bands at 1603 and 1498 cm^{-1}, related to the skeletal vibration of the aromatic ring of toluene [58][59], are attributed to the adsorption of toluene on the surface. Bands associated to the carboxylate group are present, in particular the bands around 1550, 1450 and the shoulder around 1426 cm^{-1} are related to acetate group (CH_3COO^-) and the bands around 1590, 1395 and 1375 cm^{-1} are related to the formate group (COO^-)[53][60][61]. This suggests the formation of benzoate species during the reaction. The broad and weak band around 1710 cm^{-1} is assigned to aliphatic C=O groups [62][63]. This suggests the deep oxidation and the aromatic ring cracking of the benzoate species.

At an higher wavenumber range (**Figure 3.3.2.1.2-*a***), around 2360-2330 cm^{-1}, two peaks appear which are assigned to adsorbed CO_2 [53][59][64]. They might indicate that carboxylates are further oxidized to CO_2.

3.3.2.2 Fresh $Pt^0/\gamma\text{-}Al_2O_3$

The evolution of toluene total oxidation onto fresh $Pt^0/\gamma\text{-}Al_2O_3$ catalyst surface is monitored through *in situ* transmittance FT-IR spectroscopy and the resulted spectra are reported below. As before, the wavenumber range investigated is between 1900–1300 cm^{-1}.
In **Figure 3.3.2.2.1** and **Figure 3.3.2.2.2-*b*** the dynamic evolution in the FT-IR spectra as a function of temperature is reported.

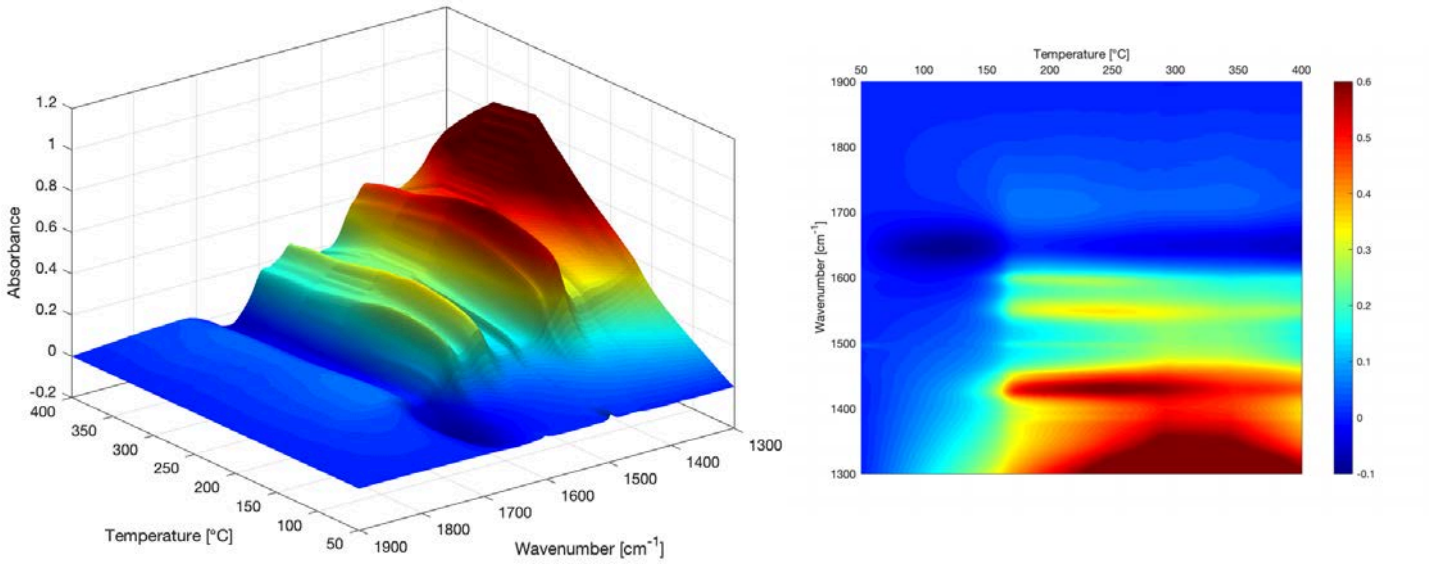

Figure 3.3.2.2.1 *Dynamic changes of the FT-IR spectra in the carbonate region with temperatures over fresh $Pt^0/\gamma\text{-}Al_2O_3$.*

The same consideration made for fresh $Pt^{\delta+}/\gamma\text{-}Al_2O_3$ stands also for the reduced one. The bands assigned to the carboxylate group are present, both acetate group (CH_3COO^-) bands around 1550, 1450 and the shoulder around 1426 cm^{-1} and the formate group (COO^-) bands around 1590, 1395 and 1375 cm^{-1} are detected after a while [53][60][61]. Therefore, the hypothesis of the formation of benzoate species during the reaction still stands. The aliphatic group broad and wide band around 1710 cm^{-1} [62][63] is also seen to support the deep oxidation of toluene and the ring cracking.
At a higher wavenumber range, around 2360-2330 cm^{-1} (**Figure 3.3.2.2.2-*a***), the bands assigned to adsorbed CO_2 appear [53][59][64], which indicate that carboxylates are further oxidized to CO_2.
In the light of the above, the oxidative state of Pt seems to be negligible in terms of reaction intermediates. This result can be explained considering the large excess of oxygen in the reaction mixture, which may oxidize the pre-reduce Pt during the test.

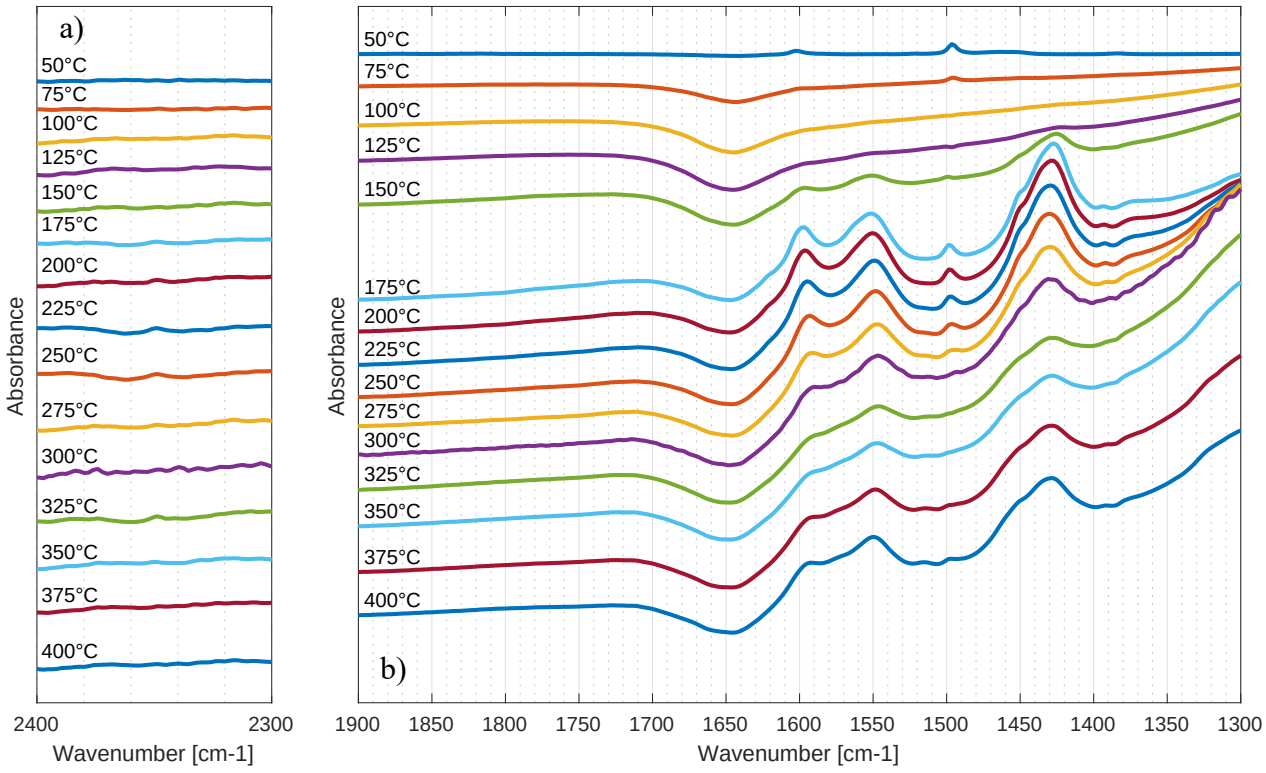

Figure 3.3.2.2.2 *FT-IR spectra each 25°C over fresh Pt^0/γ-Al_2O_3 a) between 2440-2300 cm^{-1} and b) in the carbonate range.*

3.3.2.3 Aged $Pt^{\delta+}/\gamma$-Al_2O_3

The dynamic changes taking place on fresh $Pt^{\delta+}/\gamma$-Al_2O_3 catalyst surface are monitored through *in situ* transmittance FT-IR spectroscopy and the resulted spectra are reported below.

The wavenumber range of major interest to investigate the evolution of the adsorbed species on the catalyst is between 1900–1300 cm^{-1}. In **Figure 3.3.2.3.1** and ***Figure 3.3.2.3.2-b*** the dynamic evolution in the FT-IR spectra as a function of temperature is reported.

In this case more bands show up with the evolution of the reaction together with those present during the oxidation with the fresh catalysts.

The bands at 1603 and 1498 cm^{-1} are related to the skeletal vibration of the aromatic ring of toluene due to its adsorption on the surface [58]. Bands attributed to the carboxylate group are present, in particular the acetate group (CH_3COO^-) bands around 1550, 1450 and the shoulder around 1426 cm^{-1} and the formate group (COO^-) bands around 1590, 1395 and 1375 cm^{-1} appear [53][60][61]. Confirming the possibility of the formation of benzoate species. A shoulder

around 1710 cm^{-1} associated to the aliphatic C=O group is consistent with the previous results suggesting the deep oxidation of toluene and the aromatic ring cracking [62][63].

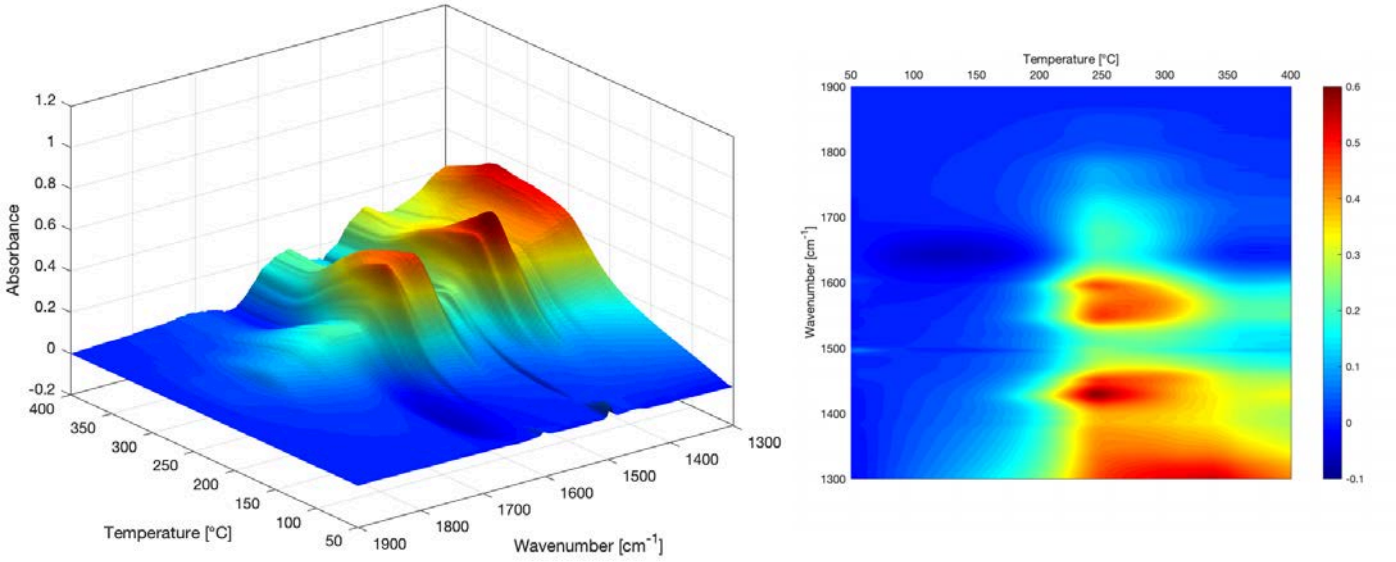

Figure 3.3.2.3.1 *Dynamic changes of the FT-IR spectra in the carbonate region with temperatures over aged $Pt^{\delta+}/\gamma$-Al_2O_3.*

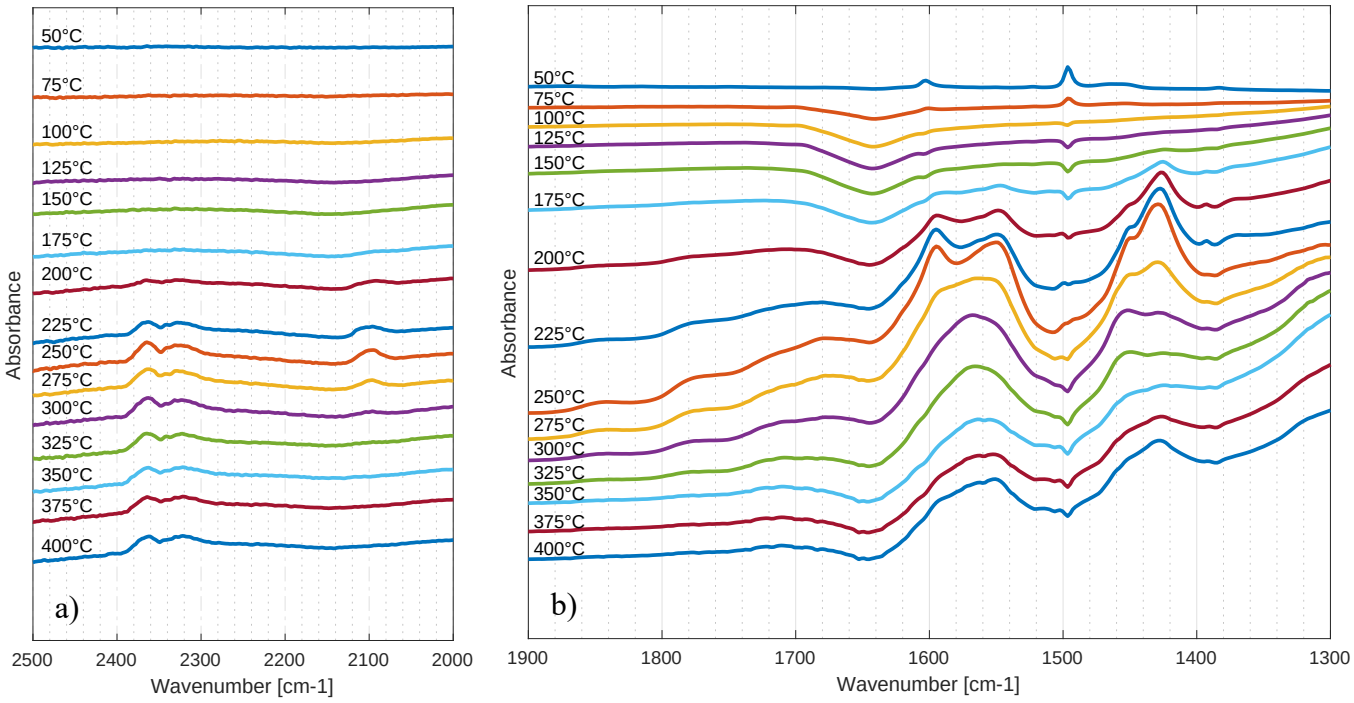

Figure 3.3.2.3.2 *FT-IR spectra each 25°C over aged $Pt^{\delta+}/\gamma$-Al_2O_3 a) between 2440-2300 cm^{-1} and b) in the carbonate range.*

Differently from before, in **Figure 3.3.2.3.2-*a***, a weak band around 2100 cm^{-1} and a shoulder 1840 cm^{-1} appear, which are assigned to CO linearly and bridged adsorbed on $Pt^{\delta+}$ [65][66]. Considering also the presence of adsorbed CO_2 weak bands at 2347 and 2326 cm^{-1} [53][59][64], further carboxylate oxidation in CO and subsequently in CO_2 can be suggested. Moreover, a shoulder is detected at 1775 cm^{-1} which is assigned to the characteristic bond of anhydride group [53][63].

3.4 *Operando* investigation

With the effort to better describe the evolution of adsorbed species on catalyst surface in function of temperature, an *operando* study is carried out. The evolution of adsorbed intermediate species derived from FT-IR spectra seen in Section 3.3.2 and toluene percentage conversion reported in Section 3.1 are analyzed together.

The semi-quantitative evolution methodology is based on absorbance measurement of the corresponding IR band according to the presence of overlapping in the spectra. Hence, the quantification of the intermediates is made by following the intensity of absorbance of bands at 1426 cm^{-1}, 1595 $cm^{-1}$and 1775 cm^{-1}, respectively for acetate, formate, anhydride adsorbed species; at 1845 cm^{-1} and 2100 cm^{-1} for CO bridge or linearly adsorbed and at 1710 cm^{-1} for C=O aliphatic group.

3.4.1 Fresh $Pt^{\delta+}/\gamma$-Al_2O_3

Toluene total oxidation over fresh $Pt^{\delta+}/\gamma$-Al_2O_3 is investigated. **Figure 3.4.1** shows the evolution of adsorbed species onto the catalyst surface taken from FT-IR (left axis) and toluene conversion (right axis) as a function of temperature.

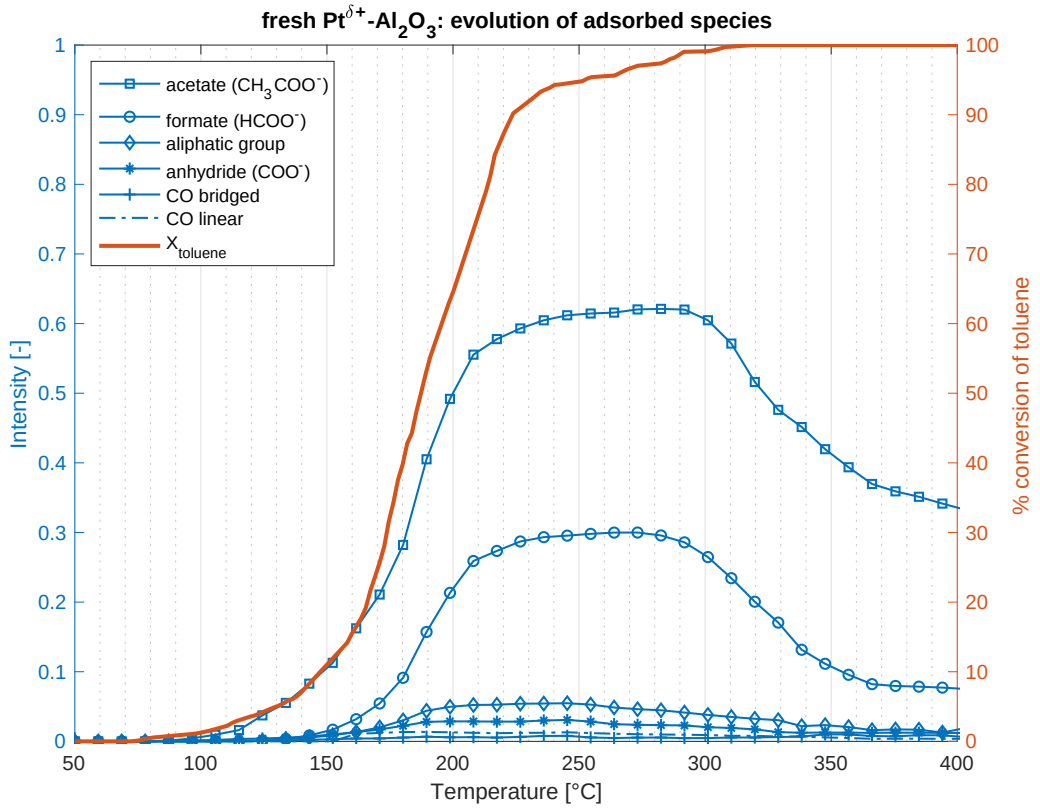

Figure 3.4.1 *Intensity of adsorbed species bands and toluene conversion over fresh $Pt^{\delta+}/\gamma$-Al_2O_3 as a function of temperature.*

The intensity of these bands is negligible when temperature is lower than 100°C, temperature at which also the toluene conversion starts. Above this temperature, the intensity of acetate species band increases remarkably with further increasing temperature from 100°C to 220°C, temperature at which the intensity reaches a plateau and the reaction shows a 60% toluene conversion. The plateau is maintained until 280°C corresponding also to 100% toluene conversion. Further increasing temperature, the intensity of this band decreases. Same consideration can be made for the intensity of the formate species band with the exception of the temperature at which intensity starts to increase. In fact, this band appears with a 30°C delay, increases until 220°C, reaches a plateau for 60°C and then decreases.
Therefore, considering the trend of the carboxylate species linked to the conversion of toluene, it can be assumed that toluene is chemically adsorbed on the catalyst surface and initially transformed into carboxylate species since its conversion starts when the carboxylates peaks appear and the conversion curve follows the same trend of the carboxylate bands intensity.
Around 160°C, also a slight increase of the aliphatic group and anhydride group bands intensity is noted, and the same behavior is shown.
The decrease seen in the acetate and formate profiles may suggest that, due to the high temperatures, sintering occurs causing a decrease in active sites.
On the other hand, the intensity of the bands associated to CO adsorbed on Pt is too weak to be detected.

3.4.2 Fresh Pt^0/γ-Al_2O_3

Toluene total oxidation over fresh Pt^0/γ-Al_2O_3 is investigated. **Figure 3.4.2**. shows the evolution of adsorbed species onto the catalyst surface taken from FT-IR (left axis) and toluene conversion (right axis) as a function of temperature.
The comments made for the fresh $Pt^{\delta+}/\gamma$-Al_2O_3 catalyst still stands for this case. In fact, as shown in **Figure 3.4.2**, the bands intensity is negligible when temperature is below 100°C, temperature at which the carboxylate species (acetate and formate) band increases markedly and the toluene conversion starts. Around 200°C a plateau is reached together with 60% toluene conversion.
With a further increase of temperature, the acetate band intensity still slightly increases, while the formate one is quite stable. Anyway, both bands intensity decreases from 260°C, temperature at which 100% of toluene conversion is reached. Hence, the assumption that toluene after the adsorption is converted into carboxylate species is valid.
After 150°C, the intensity of aliphatic and anhydride group bands slightly increases, as before, with a lower intensity compared to the ones of carboxylate species but showing the same trend
Also in this case, the intensity of the bands associated to CO adsorbed on Pt is too weak to be detected.

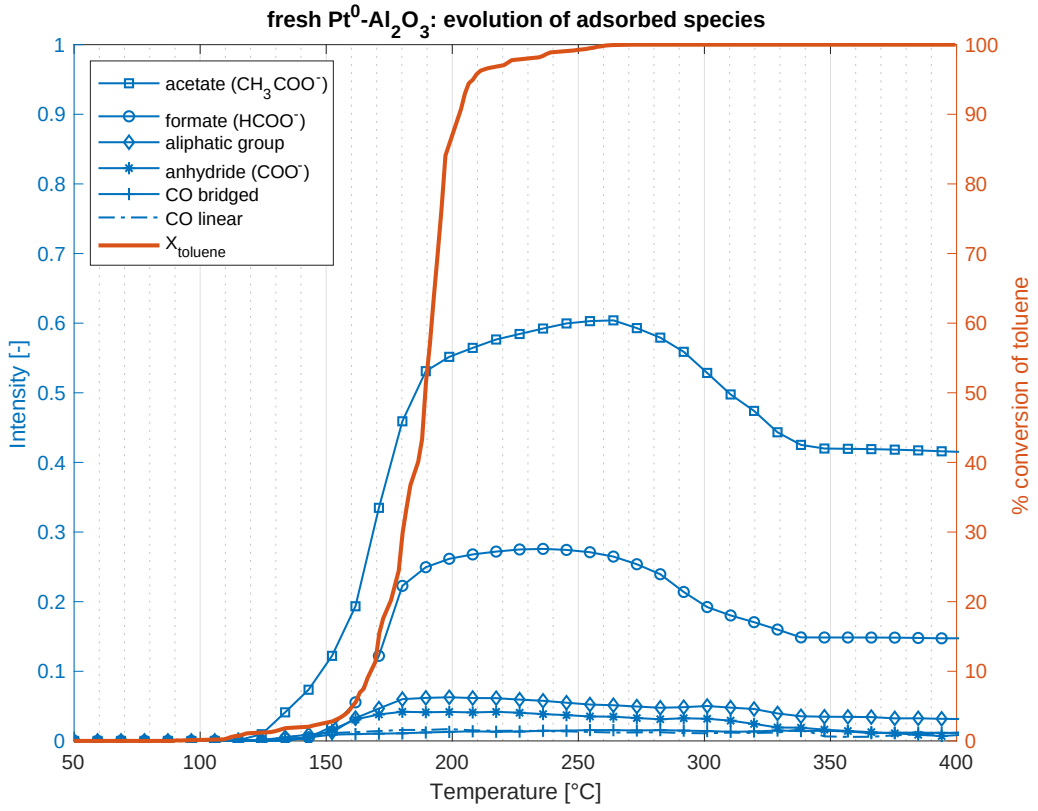

Figure 3.4.2 *Intensity of adsorbed species bands and toluene conversion over fresh Pt^0/γ-Al_2O_3 as a function of temperature.*

3.4.3 Aged $Pt^{\delta+}/\gamma$-Al_2O_3

Toluene total oxidation over aged $Pt^{\delta+}/\gamma$-Al_2O_3 is investigated. **Figure 3.4.3**. shows the evolution of adsorbed species onto the catalyst surface taken from FT-IR (left axis) and toluene conversion (right axis) as a function of temperature.

In this case, as seen in Section 3.3.2, results deviate from what is obtained with the fresh catalysts.

For all bands, the intensity becomes relevant from 120°C, temperature at which also the toluene conversion starts, and increases remarkably with further increasing temperature as far as 250°C. In fact, at 250°C the intensities curves reach their maximum value and toluene conversion is around 95%. After 250°C, with a further increase of temperature, the bands intensity decreases. It should be noticed that with the aged catalyst, the intensity of aliphatic and anhydride group bands is higher compared to the fresh catalysts and the intensity of the bands associated to CO adsorbed on Pt is detected.

The carboxylate group bands (acetate and formate) intensity starts to increase before the other species intensity, which display a delay. This can support the assumption that benzoate species are decomposed into aliphatic carboxylate species and then to anhydride species.

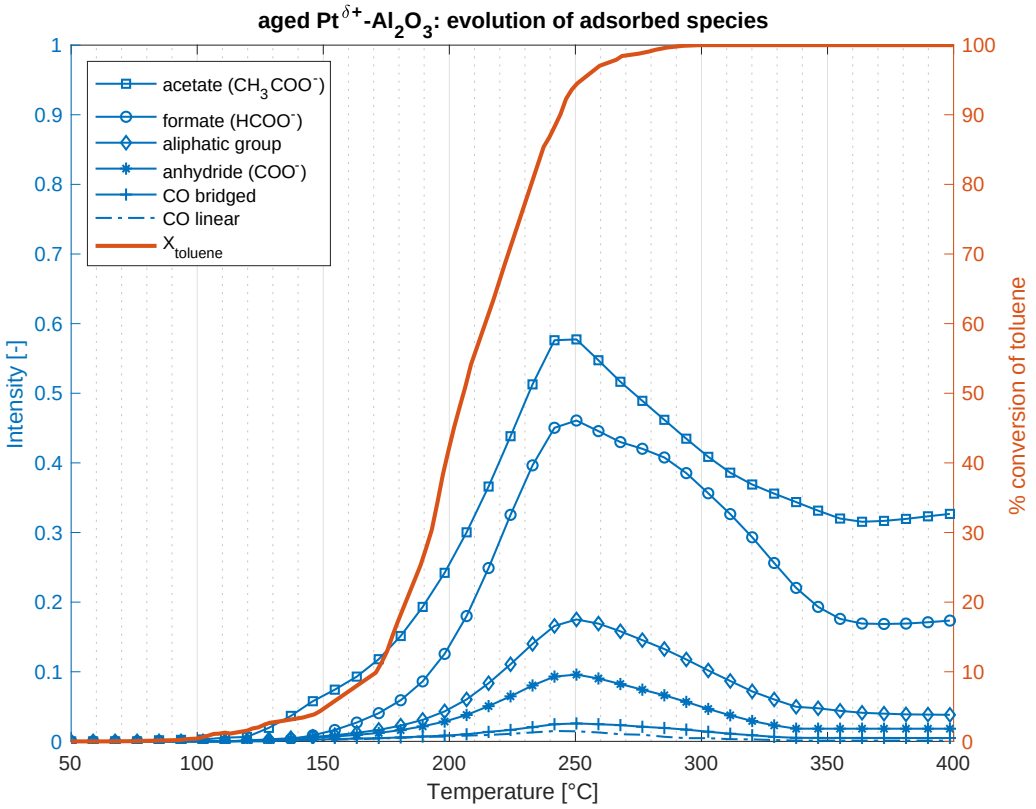

Figure 3.4.3 *Intensity of adsorbed species bands and toluene conversion over fresh $Pt^{\delta+}$-Al_2O_3 as a function of temperature.*

3.5 *Discussion*

In the light of the above results, the following considerations can be made.

First of all, the obtained data show that the effect of the oxidation state of Pt is negligible in the toluene combustion. In fact, both the toluene conversion (**Figure 3.1.1**) and the yield into CO_2 (**Figure 3.1.2**) curves on fresh $Pt^{\delta+}$ and fresh Pt^0 catalysts outline very close T_{50} (temperature corresponding to 50% of toluene conversion and yield into CO_2, ***Table 3.1.1***), which is an indicative parameter to compare the activity of different catalysts. Moreover, the FT-IR spectra collected during the experiments related to those catalysts display very similar behaviors (**Figure 3.3.2.1.2-Figure 3.3.2.2.2**).

On the other hand, there are differences between the fresh and the aged catalysts. Concerning the toluene conversion (**Figure 3.1.1**) and the yield into CO_2 (**Figure 3.1.2**), the aged one shows a 20°C higher T_{50} (***Table 3.1.1***), denoting a lower activity of this catalyst compared to the fresh one. This is also supported by the fact that the reaction on this catalyst presents the highest calculated apparent activation energy (***Table 3.2.2.1***).

Consistently with above considerations, the oxidation state does not affect the results in this analysis. Instead, two different behaviors are recognized in the *operando* investigation depending on which catalyst is used, fresh (**Figure 3.4.1-Figure 3.4.2**) or aged (**Figure 3.4.3**). Given that, from now on both fresh $Pt^{\delta+}$ and fresh Pt^0 catalysts will be referred as fresh catalyst (in a general way).

All the investigations made, and in particular the *operando* FT-IR analysis, are very useful to put forward an assumption of the reaction cycle for toluene oxidation over $Pt/\gamma\text{-}Al_2O_3$, which is presented in **Figure 3.5.1**.

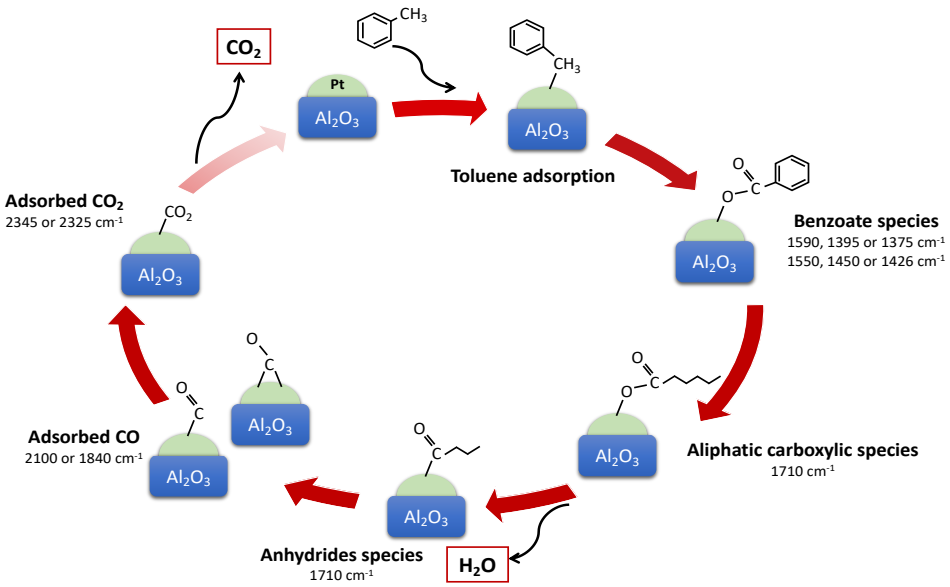

Figure 3.5.1 *Proposed reaction scheme for the catalytic oxidation of toluene onto Pt/γ-Al2O3*

In the proposed mechanism, toluene is firstly adsorbed on the active sites of Pt-γAl_2O_3 and reacts with adsorbed O_2 to form benzoate species. Benzoate species are then decomposed into aliphatic carboxylic species due to ring cracking, which are in their turn converted in anhydrides. Afterwards, anhydrides are converted into adsorbed CO species and H_2O. At last, adsorbed CO species reacts with adsorbed O_2 to give CO_2, which, once de-adsorbed, leaves the active site to the incoming reactants, completing the cycle.
The hypnotized reaction steps are schematically reported below, in **Table 3.5.1**.

Table 3.5.1 *Total toluene oxidation onto Pt/γ-Al_2O_3: hypothesis of reaction steps.*

$C_6H_5 - CH_3 + \sigma \rightarrow \sigma[C_6H_5 - CH_3]\backslash$ $O_2 + \sigma \rightarrow \sigma[O_2]$	Reactant adsorption
$2\,\sigma[C_6H_5 - CH_3] + 4\,\sigma[O_2] \rightarrow 2\,\sigma[C_6H_5 - CO_2] + 4\,\sigma[H_2O]$	Toluene oxidation to benzoate species
$\sigma[C_6H_5 - CO_2] \rightarrow \sigma[C_6H_5CO_2]$	Ring cracking of benzoate species
$4\,\sigma[C_6H_5CO_2] + 2\,\sigma[O_2] \rightarrow 4\,\sigma[C_5H_4CO] + 2\,\sigma[H_2O] + 4\,\sigma[CO]$	Aliphatic species converted to anhydride, CO and H_2O
$2\,\sigma[CO] + \sigma[O_2] \rightarrow 2\,\sigma[CO_2]$	Oxidation of adsorbed CO to CO_2
$\sigma[CO_2] \rightarrow CO_2 + \sigma$ $\sigma[H_2O] \rightarrow H_2O + \sigma$	CO_2 and H_2O de-adsorption

Other speculations on the reaction mechanism can be made looking at the trends of intensity evolution curves of the adsorbed species on fresh and aged catalysts.
Referring to the benzoate species intensities on the fresh catalyst (**Figure 3.4.1**-**Figure 3.4.2**), they are almost the only intermediates shown with the *in situ* FT-IR, meaning that they represent the most relevant intermediates in toluene oxidation. This result confirms the studied made by S. Zhao et al. [28] and Z. Rui et al. [54] which reported that the benzoate species were the most important intermediates in toluene total oxidation on Pd-Co based and Pt/TiO_2 catalysts, respectively.

In addition, the fact that these species show a plateau can indicate that the decomposition of the benzoate species represents the rate determining step of the reaction mechanism, consistently with other study in literature [54]. In fact, once adsorbed, toluene immediately reacts with adsorbed O_2 to give benzoate species, while the conversion of benzoate species to aliphatic carboxylic species presents a slower reaction rate (the slowest). Once obtained the aliphatic carboxylic species, the reaction mechanism proceeds quickly to the ultimate oxidation products, so that they do not accumulate on the surface. Therefore, the FT-IR is not able to detect properly their evolution.

In view of this, the plateau shows by the benzoate species can be considered as an evidence of achievement of active sites saturation on the catalyst. In fact, since the benzoate species decomposition rate is low and the other steps are very fast, once one benzoate is converted, the next steps proceed so fast to let the active sites free almost immediately. Now, the newly free active sites are being rapidly taken by toluene and O_2, which quickly react to give a benzoate specie. Thus, the FT-IR detects only benzoate species and low amount of others.

Lastly, the fact that around 280°C the benzoates intensity starts to decrease can indicate a reduction of active sites on the surface.

On the other hand, on the aged catalyst the reaction proceeds slower compared to the fresh one because of the lower performance, as expected, which also results in a different trend showed by the adsorbed species bands intensity evolution (**Figure 3.4.3**). In particular, the benzoates intensity reaches a maximum (instead of a plateau) because of the presence of other species on the surface. Especially, all the reaction steps show lower rates which can be outlined by the fact that not only benzoate species, but also aliphatic carboxylic species, anhydride species and adsorbed CO are seen by the FT-IR.

The explanation of this adsorbed species behavior may stand in the fact that, since the reaction steps after the decomposition of benzoate species are slower than on the fresh catalysts, the corresponding intermediates remain adsorbed on the active site for more time before being converted in something else. Thus, they accumulate on the surface making the FT-IR able to detect them.

Conclusions

In this work several *operando* FT-IR spectroscopic measurements – through temperature ramping tests – have been performed to investigate the main surface reaction mechanism of toluene total oxidation (chosen as model reaction) occurring onto a commercial 1%wt Pt/γ-Al_2O_3 catalyst. The effect of Pt oxidative (δ+ and 0) state and sintering on the reaction have been also considered.

A preliminary investigation on catalysts performance has been pointed out. It was shown that the impact of the Pt oxidative state has been negligible: the reaction – always performed with a reacting mixture of 800 ppm toluene/10% O_2/He – on both $Pt^{\delta+}$ and Pt^0 catalysts reached 50% of toluene conversion around 190°C. Instead sintering – aged $Pt^{\delta+}$ catalyst – caused a decrease in catalyst activity suggesting a lower amount of active sites on the surface. 50% of toluene were converted around 210°C.

Nevertheless, a toluene conversion higher than 95% has been achieved at 300°C for all cases.

Operando FT-IR study has led to a hypothesis of the main reaction cycle: toluene, after being adsorbed over Pt/γ-Al_2O_3 active sites, has been sequentially oxidized to benzoate, aliphatic carboxylate species, CO and finally CO_2.

In addition, the decomposition of benzoate species (formate and acetate) – ring cracking – has been found to be the rate determining step of the reaction since they were accumulated on catalyst surface. This is in agreement with previous studies on toluene total oxidation reported in the literature.

However, the identification of the actual intermediates hasn't been possible with the adopted operating conditions and set up. In fact, to simulate automotive exhaust catalysts conditions, the catalyst weight/reactant ratio (w/F) has been kept as lower as possible, leading to sensitivity problems with the online analysis instrumentation: the amount of intermediates were too low to be detected by the MS. Moreover, the discrimination between active/inactive species in the reaction mechanism hasn't been possible since the performed tests do not provide this kind of information.

To overcome these limitations, future studies could stress the attention on two main objectives. On one hand, set up changing should be considered in order to obtain more reliable measurements of product composition. An option could be using the GC, not only to detect the occurrence of leaks but also to evaluate the outer stream composition.

On the other hand, other tests can be performed to develop a more detailed study on the catalytic system. In this regard, interesting results are obtained combining *operando* spectroscopy with

steady-state isotopic transient kinetics analysis (SSITKA). In particular, this spectro-kinetic method allows to distinguish between participating surface reaction intermediates and inactive surface spectators analyzing the system response to an isotopic switch in the reactant mixture. In this way, a complete reaction mechanism – comprehensive of main reaction cycle and determination of inactive species reacting outside it – can be outlined and sequentially improvement on the activity selectivity of the catalyst and, in general, on the process can be made.

Bibliography

[1] B. Zhang and D. S. Su, "Advanced Electron Microscopy and Spectroscopy for Catalysis", *ChemCatChem*, vol. 7, no. 22, pp. 3598–3600, 2015.
[2] J. Hagen, *Industrial catalysis: a practical approach*, Wiley-VCH, Weinheim. 1999.
[3] H. F. Rase, *Handbook of commercial catalyst*. New York: CRC Press, 2000.
[4] B. M. Weckhuysen, "Determining the active site in a catalytic process: Operando spectroscopy is more than a buzzword", *Physical Chemistry Chemical Physics*, vol. 5, no. 20, p. 4351, 2003.
[5] O. N. Temkin, *Homogeneous catalysis with metal complexes: kinetic aspects and mechanism*. Chichester: Wiley, 2012.
[6] G. Hertl, H. Knozinger, and J.Weitkamp, *Handbook of heterogeneous catalysis*. Weinheim: Wiley-VCH.
[7] A. F. Schmidt, A. A. Kurokhtina, and E. V. Larina, "Kinetic aspects of operando studies: state-of-the-art and unexplored possibilities" , *Mendeleev Communications*, vol. 27, no. 3, pp. 213–223, 2017.
[8] M. Jacoby, "Chemical and engineering news", 04-May-1998.
[9] R. Schlögl, "Heterogene Katalysatoren - fundamental betrachtet", *Angewandte Chemie*, vol. 127, no. 11, pp. 3531–3589, 2015.
[10] B. M. Weckhuysen, "Snapshots of a working catalyst: possibilities and limitations of in situ spectroscopy in the field of heterogeneous catalysis", *Chemical Communications*, no. 2, pp. 97–110, 2002.
[11] R. P. Eischens, W. A. Pliskin, and S. A. Francis, "Infrared Spectra of Chemisorbed Carbon Monoxide", *The Journal of Chemical Physics*, vol. 22, no. 10, pp. 1786–1787, 1954.
[12] J. E. Mapes and R. P. Eischens, "The Infrared Spectra of Ammonia Chemisorbed on Cracking Catalysts", *The Journal of Physical Chemistry*, vol. 58, no. 12, pp. 1059–1062, 1954.
[13] M. A. Bañares and I. E. Wachs, "Molecular structures of supported metal oxide catalysts under different environments: Molecular structures of supported metal oxide catalysts", *Journal of Raman Spectroscopy*, vol. 33, no. 5, pp. 359–380, 2002.
[14] N. E. Tsakoumis, A. P. E. York, D. Chen, and M. Rønning, "Catalyst characterisation techniques and reaction cells operating at realistic conditions; towards acquisition of kinetically relevant information", *Catalysis Science & Technology*, vol. 5, no. 11, pp. 4859–4883, 2015.
[15] A. V. Gaikwad and G. Rothenberg, "In-situ UV-visible study of Pd nanocluster formation in solution", *Physical Chemistry Chemical Physics*, vol. 8, no. 31, p. 3669, 2006.
[16] J. A. Creighton and D. G. Eadon, "Ultraviolet–visible absorption spectra of the colloidal metallic elements", *J. Chem. Soc., Faraday Trans.*, vol. 87, no. 24, pp. 3881–3891, 1991.
[17] C. Lv *et al.*, "Pd3 cluster catalysis: Compelling evidence from in operando spectroscopic, kinetic, and density functional theory studies", *Nano Research*, vol. 9, no. 9, pp. 2544–2550, Sep. 2016.
[18] X. L. Wang *et al.*, "Operando NMR spectroscopic analysis of proton transfer in heterogeneous photocatalytic reactions", *Nature Communications*, vol. 7, no. 1, 2016.
[19] M. A. Bañares, "Operando methodology: combination of in situ spectroscopy and simultaneous activity measurements under catalytic reaction conditions", *Catalysis Today*, vol. 100, no. 1–2, pp. 71–77, Feb. 2005.
[20] M. A. Bañares, M. O. Guerrero-Pérez, J. L. G. Fierro, and G. G. Cortez, "Raman spectroscopy during catalytic operations with on-line activity measurement (operando spectroscopy): a method for understanding the active centres of cations supported on porous materials", *J. Mater. Chem.*, vol. 12, no. 11, pp. 3337–3342, 2002.
[21] M. O. Guerrero-Pérez and M. A. Bañares, "Operando Raman study of alumina-supported Sb–V–O catalyst during propane ammoxidation to acrylonitrile with on-line activity measurement", *Chemical Communications*, no. 12, pp. 1292–1293, 2002.

[22] J. W. Ward, “The nature of active siteson zeolites V. In situ spectrocopic observations of hydrogen Y zeolite during cumene cracking.”, *J. Catal.*, vol. 11, pp. 259–273, 1968.
[23] J.F. Joly, N. Zanier-Szydlowski, S. Colin, F. Raatz, J. Saussey, and J.C. Lavalley, “Infrared in situ characterization of HY zeolite acid sites during cyclohexene transformation”, *Catalysis Today*, vol. 9, no. 1–2, pp. 31–38, 1991.
[24] P. Maets, J. Saussey, J. C. Lavalley, and R. Touroude, “Hydrogenation of but-1-yne on platinum/silica catalysts: an in situ dynamic infrared study”, *J. Catal.*, vol. 147, pp. 48–56, 1994.
[25] J. Saussey and F. Thibault-Starzyk, *Infrared spectroscopy: classical methods*. San Diego: American Scientific Publishers, 2004.
[26] R. K. Arvela, N. E. Leadbeater, M. S. Sangi, V. A. Williams, P. Granados, and R. D. Singer, “A Reassessment of the Transition-Metal Free Suzuki-Type Coupling Methodology”, *The Journal of Organic Chemistry*, vol. 70, no. 1, pp. 161–168, 2005.
[27] Á. Gordillo, E. de Jesús, and C. López-Mardomingo, “Consecutive palladium-catalyzed Hiyama–Heck reactions in aqueous media under ligand-free conditions”, *Chemical Communications*, no. 39, p. 4056, 2007.
[28] S. Zhao, K. Li, S. Jiang, and J. Li, “Pd–Co based spinel oxides derived from pd nanoparticles immobilized on layered double hydroxides for toluene combustion”, *Applied Catalysis B: Environmental*, vol. 181, pp. 236–248, 2016.
[29] A. Urakawa, “Trends and advances in Operando methodology”, *Current Opinion in Chemical Engineering*, vol. 12, pp. 31–36, 2016.
[30] J. R. Morris, J. N. Russell, and C. J. Karwacki, “An Operando View of the Nanoscale”, *The Journal of Physical Chemistry Letters*, vol. 6, no. 24, pp. 4923–4926, 2015.
[31] A. Chakrabarti *et al.*, “A decade+ of operando spectroscopy studies”, *Catalysis Today*, vol. 283, pp. 27–53, 2017.
[32] F. Tao *et al.*, “Reaction-Driven Restructuring of Rh-Pd and Pt-Pd Core-Shell Nanoparticles”, *Science*, vol. 322, no. 5903, pp. 932–934, 2008.
[33] S Vendelbo *et al.*, “In situ HRTEM of a Catalyst Using a Nanoreactor at 1 bar”, *Microscopy and Microanalysis*, vol. 17, no. S2, pp. 536–537, 2011.
[34] J. Ryczkowski, “IR spectroscopy in catalysis”, *Catalysis Today*, vol. 68, no. 4, pp. 263–381, 2001.
[35] A. F. Schmidt, A. Al-Halaiqa, V. V. Smirnov, and A. A. Kurokhtina, “State of palladium in ligandless catalytic systems for the Heck reaction of nonactivated bromobenzene”, *Kinetics and Catalysis*, vol. 49, no. 5, pp. 638–643, 2008.
[36] C. Amatore and A. Jutand, “Anionic Pd(0) and Pd(II) Intermediates in Palladium-Catalyzed Heck and Cross-Coupling Reactions”, *Accounts of Chemical Research*, vol. 33, no. 5, pp. 314–321, 2000.
[37] G. C. Bond and R. H. Cunningham, “Alkane Transformations on Supported Platinum Catalysts”, *Journal of Catalysis*, vol. 166, no. 2, pp. 172–185, 1997.
[38] H. Huang, Y. Xu, Q. Feng, and D. Y. C. Leung, “Low temperature catalytic oxidation of volatile organic compounds: a review”, *Catalysis Science & Technology*, vol. 5, no. 5, pp. 2649–2669, 2015.
[39] M. S. Kamal, S. A. Razzak, and M. M. Hossain, “Catalytic oxidation of volatile organic compounds (VOCs) – A review”, *Atmospheric Environment*, vol. 140, pp. 117–134, 2016.
[40] P. Le Cloirec, *Les composés organiques volatils dans l’environnement. Technique et Documentation*. Paris: Lavoisier Eds, 1998.
[41] L.-Y. Lin, C. Wang, and H. Bai, “A comparative investigation on the low-temperature catalytic oxidation of acetone over porous aluminosilicate-supported cerium oxides”, *Chemical Engineering Journal*, vol. 264, pp. 835–844, 2015.
[42] M. Duplancic, V. Tomasic, S. Kurajica, I. Minga, and K. M. Valkaj, “A comparative study of toluene oxidation on different metal oxides”, *Chemical Engineering Transactions*, pp. 889–894, 2017.
[43] F. Zhang *et al.*, “Tailoring the Oxidation Activity of Pt Nanoclusters via Encapsulation”, *ACS Catalysis*, vol. 5, no. 2, pp. 1381–1385, 2015.
[44] Y. Li *et al.*, “Pt-based structured catalysts on metallic supports synthesized by electroless plating deposition for toluene complete oxidation”, *Catalysis Today*, vol. 281, pp. 542–548, 2017.

[45] V.P. Santos, S. A. C. Carabineiro, P. B. Tavares, M. F. R. Pereira, J. J. M. Órfão, and J. L. Figueiredo, "Oxidation of CO, ethanol and toluene over TiO2 supported noble metal catalysts", *Applied Catalysis B: Environmental*, vol. 99, no. 1–2, pp. 198–205, 2010.
[46] L. Matějová, P. Topka, K. Jirátová, and O. Šolcová, "Total oxidation of model volatile organic compounds over some commercial catalysts", *Applied Catalysis A: General*, vol. 443–444, pp. 40–49, Nov. 2012.
[47] X. Liu, Q. Zhang, P. Ning, T. Tang, J. Hu, and W. Su, "One-pot synthesis of mesoporous Al2O3 -supported Pt-Pd catalysts for toluene combustion", *Catalysis Communications*, vol. 115, pp. 26–30, 2018.
[48] N. Radic, B. Grbic, and A. Terlecki-Baricevic, "Kinetics of deep oxidation of n-hexane and toluene over Pt/Al2O3 catalysts", *Applied Catalysis B: Environmental*, vol. 50, no. 3, pp. 153–159, 2004.
[49] Z. Rui, C. Chen, Y. Lu, and H. Ji, "Anodic Alumina Supported Pt Catalyst for Total Oxidation of Trace Toluene", *Chinese Journal of Chemical Engineering*, vol. 22, no. 8, pp. 882–887, 2014.
[50] G. Busca, "Infrared studies of the reactive adsorption of organic molecules over metal oxides and of the mechanisms of their heterogeneously-catalyzed oxidation", *Catalysis Today*, vol. 27, no. 3–4, pp. 457–496, 1996.
[51] G. da Silva, C.-C. Chen, and J. W. Bozzelli, "Toluene Combustion: Reaction Paths, Thermochemical Properties, and Kinetic Analysis for the Methylphenyl Radical + O_2 Reaction", *The Journal of Physical Chemistry A*, vol. 111, no. 35, pp. 8663–8676, 2007.
[52] S. Besselmann, E. Löffler, and M. Muhler, "On the role of monomeric vanadyl species in toluene adsorption and oxidation on V2O5/TiO2 catalysts: a Raman and in situ DRIFTS study", *Journal of Molecular Catalysis A: Chemical*, vol. 162, no. 1–2, pp. 401–411, 2000.
[53] H. Sun, Z. Liu, S. Chen, and X. Quan, "The role of lattice oxygen on the activity and selectivity of the OMS-2 catalyst for the total oxidation of toluene", *Chemical Engineering Journal*, vol. 270, pp. 58–65, 2015.
[54] Z. Rui, M. Tang, W. Ji, J. Ding, and H. Ji, "Insight into the enhanced performance of TiO2 nanotube supported Pt catalyst for toluene oxidation", *Catalysis Today*, vol. 297, pp. 159–166, 2017.
[55] A. Gorczyca *et al.*, "Monitoring Morphology and Hydrogen Coverage of Nanometric Pt/γ-Al2O3 Particles by In Situ HERFD-XANES and Quantum Simulations", *Angewandte Chemie International Edition*, 2014.
[56] L. D. Schmidt, *The engineering of chemical reactions*, 2nd edition. Oxford University press, 1998.
[57] K. Everaert, "Catalytic combustion of volatile organic compounds", *Journal of Hazardous Materials*, vol. 109, no. 1–3, pp. 113–139, 2004.
[58] M. D. Hernández-Alonso, I. Tejedor-Tejedor, J. M. Coronado, and M. A. Anderson, "Operando FTIR study of the photocatalytic oxidation of methylcyclohexane and toluene in air over TiO2–ZrO2 thin films: Influence of the aromaticity of the target molecule on deactivation", *Applied Catalysis B: Environmental*, vol. 101, no. 3–4, pp. 283–293, 2011.
[59] Z. Zhu, F. Liu, and W. Zhang, "Fabricate and characterization of Ag/BaAl2O4 and its photocatalytic performance towards oxidation of gaseous toluene studied by FTIR spectroscopy", *Materials Research Bulletin*, vol. 64, pp. 68–75, 2015.
[60] X. Wu, L. Zhang, D. Weng, S. Liu, Z. Si, and J. Fan, "Total oxidation of propane on Pt/WOx/Al2O3 catalysts by formation of metastable Ptδ+ species interacted with WOx clusters", *Journal of Hazardous Materials*, vol. 225–226, pp. 146–154, 2012.
[61] C. Belver, M. J. López-Muñoz, J. M. Coronado, and J. Soria, "Palladium enhanced resistance to deactivation of titanium dioxide during the photocatalytic oxidation of toluene vapors", *Applied Catalysis B: Environmental*, vol. 46, no. 3, pp. 497–509, 2003.
[62] H. Einaga, K. Mochiduki, and Y. Teraoka, "Photocatalytic Oxidation Processes for Toluene Oxidation over TiO2 Catalysts", *Catalysts*, vol. 3, no. 1, pp. 219–231, 2013.
[63] J. Wu, Q. Xia, H. Wang, and Z. Li, "Catalytic performance of plasma catalysis system with nickel oxide catalysts on different supports for toluene removal: Effect of water vapor", *Applied Catalysis B: Environmental*, vol. 156–157, pp. 265–272, 2014.
[64] H. Chen, Z. Rui, and H. Ji, "Monolith-Like TiO_2 Nanotube Array Supported Pt Catalyst for HCHO Removal under Mild Conditions", *Industrial & Engineering Chemistry*

Research, vol. 53, no. 18, pp. 7629–7636, 2014.
[65] A. Bourane, S. Derrouiche, and D. Bianchi, “Impact of Pt dispersion on the elementary steps of CO oxidation by O2 over Pt/Al2O3 catalysts”, *Journal of Catalysis*, vol. 228, no. 2, pp. 288–297, 2004.
[66] M. Paulis, H. Peyrard, and M. Montes, “Influence of Chlorine on the Activity and Stability of Pt/Al2O3 Catalysts in the Complete Oxidation of Toluene”, *Journal of Catalysis*, vol. 199, no. 1, pp. 30–40, 2001.